Mohamed Khider University of Biskra
Faculty of Science and Technology
Department of Mechanical Engineering

Master Dissertation

Field: Sciences and Techniques
Sector: Metallurgy
Speciality: Metallurgy Engineering

Ref.:

Presented and supported by:

BEN AMEUR Mohamed Cherif

On: June, 28, 2022

Protection against Corrosion of API 5L X70 carbon steel pipelines in acidic media (H_2SO_4) by aloe vera gel as an eco-friendly inhibitor

Protection contre la corrosion des canalisations en acier au carbone API 5L X70 en milieu acide (H_2SO_4) par le gel d'aloe vera comme inhibiteur écologique

---

Jury:

Pr.	Boumerzoug Zakaria	Pr	University of Biskra	President
Dr.	Bentrah Hamza	MCA	University of Biskra	Reporter
Dr.	Chouia Fateh	MCA	University of Biskra	Examiner

Academic year: 2021- 2022

DEDICATION

The price of success is hard work, dedication to the job at hand, and the determination that whether we win or lose, we have applied the best of ourselves to the task at hand

I dedicate My effort to

My sweet and loving Father & Mother

Whose affection, love, encouragement, and prayers of the day and night made me able to achieve such success

Also, I would like to give special thanks to my grandma, my parents, and to my friends (AOUN Ala Eddine, Soltane Sifeddine) for the support through writing this thesis

Acknowledgement

It is a pleasure for me to thank my supervisor, Dr. BENTRAH Hamza, for his continued support of my research and work, and for his immense knowledge. I greatly appreciated his guidance throughout the entire research and writing of this dissertation.

Also, I wish to thank Professor BOUMERZOUG Zakaria, the president of my jury, and CHOUIA Fatah, the examiner, for serving as my committee members and for their brilliant comments and suggestions.

Table of Contents

List of Tables

Chapter I

Chapter II

Chapter III

List of Figures

Chapter I

Chapter II

Chapter III

List of Equations

Chapter I

Chapter II

List of Abbreviations

AVG: Aloe Vera Gel

C: Inhibitor concentration

M: Molarity

Ki: Potassium iodide

Icorr: corrosion current density

Icorr(inh): corrosion current density in presence of inhibitor

bc: cathodic coefficient

ba: anodic coefficient

Ecorr: corrosion potential

L: inductance

OCP: Open Circuit Potential

NHE: Normal Hydrogen Electrode

API: American Petroleum Institute

Rs: Resistance of solution

Rt: Resistance of charge transfer

ṛ t : R e s of i charge transfer in presence of inhibitor

EIS: Electrochemical Impedance Spectroscopy

q_{EIS}: inhibition efficiency calculated from ESI

q_{Pol}: inhibition efficiency calculated from potentiodynamic polarization

CPE: Constant Phase Element

General Introduction

Pipelines are primarily used by the petroleum industry, where corrosion factors cause countless pipeline failures every year that result in pollution, deterioration of transportation and equipment, and significant production losses [1].

By 2016, *the National Association of Corrosion Engineers (NACE), a part of International Measures of Prevention, Application and Economic of Corrosion Technologies Study (IMPACT),* conducted a study about the cost of corrosion globally of the year 2013 which is estimated to be US$2.5 trillion, equivalent to 3.4% of the global GDP. Relying on corrosion inhibitors, it is possible to save 15% up to 35% of the corrosion costs, and that can approximately be between US$375 and US$875 billion annually on a global basis [2].

The acid treatment is not to date. *Herman Frasch* discove
a chemist at *Standard Oil Co.'s Solar Refinery of Lima, Ohio* made the first acid treatment experiment by using HCL (Hydrochloric acid) that interacts with limestone producing carbon dioxide (gas) and calcium chloride (salt that is soluble in water), which are removed from the formation by the production pressure of the well fluids after. This experiment done had achieved a major successful result by increasing the production of oil up to 300% and 400% for the gas. 33 years after, another significant achievement had been recorded using acid in oilwell by the Gypsy oil co. The operation solved the problem of scale in pipelines by using an inhibitor to protect the steel mills from corrosion [3].

In the oil and gas industry, the majority of the corrosion inhibitors used have negative impacts, posing a threat to the eco-system, and classified toxic substances such as inorganic compounds**.** like nitrite (NO_2) [4], chromates **(**CrO) [5], molybdate (MoO) [6], and phosphate (PO_4) [7].

As environmental agencies have established strict regulations and rules for toxicity, biodegradability, and bioabsorption, the inhibiting agents must be evaluated in relation to their impact on human health, safety, and the environment [8]. The establishment of these regulations prompted scientists to seek alternative corrosion inhibitors [9].

There are a wide range of organic compounds available in nature that are cost-effective, accessible, eco-friendly, reproducible, and can be easily extracted from trees and plants. Many of these natural compounds are effective against corrosion with high inhibition efficiency (IE) [10].

Several studies had been conducted about organic green inhibitors which are eco-friendly such as *Dardagan Fruit* extract with inhibition efficiency of 92% [11], *Gum Arabic* (GA*)* with inhibition efficiency of 92% [12], *Davidia involucrata* leaf extract (DLE) was 90% [13], and *Ficus tikoua* leaves extract was 95.8% [14].

The selected substance in this research is an organic gel extracted from the aloe vera plant as a green inhibitor. the extracted gel from the leaves of the plant is transparent and sticky in texture.

The objective of this study is to test the efficiency of Aloe vera extracted gel as an eco-friendly inhibitor against the corrosion of API 5L X70 carbon steel in sulfuric acid (H_2SO_4) media by electrochemical methods and surface analyses.

Chapter I

Chapter I is addressed to the introduction and literature review on corrosion of carbon steel, corrosion types in hydrocarbon pipelines, corrosion of carbon steel in acidic medium, acid injection (acidizing) and reservoir formation as the first part.

The second part is addressed to literature review on protection of carbon steel against corrosion in acidic media by corrosion Inhibitors, Inhibition Mechanism of organic inhibitors.

The third part is addressed to literature review on Eco-friendly inhibitors for carbon steel in acidic media, Aloe Vera, chemical composition and molecular structure of Aloe Vera Gel.

Chapter II

The goal of this chapter is to provide a brief overview of electrochemical techniques and surface analysis used in this study to give essential information about how the experiment was conducted and to investigate the inhibition efficiency of Aloe Vera Gel.

Chapter III

As a general overview in this chapter, the results obtained from the electrochemical techniques and the surface analysis of API 5L X70 steel is divided into:

The corrosion behavior of API 5L X70 steel has been studied in 0.5M H_2SO_4 acid solution to determine the electrochemical parameters, and also to understand the corrosion mechanism API 5L X70 steel in acid solution.

Aloe Vera Gel has been investigated by electrochemical impedance spectroscopy, potentiodynamic polarization, and surface analyses by Optical Microscope (OM) in sulfuric acid solution for understanding the inhibition mechanism of AVG.

Synergetic effect of the combination AVG and iodide ions (I^-) in sulfuric acid solution has been studied by electrochemical techniques and surface analyses to understand the inhibition efficiency of the system AVG + iodide ions.

Chapter I : Introduction and review of literature

I.1 Corrosion of carbon steel (API 5L X70) in acidic media for the oil and gas industry

I.1.1 Corrosion

Corrosion is a process in which a high-energy (processed) metal or metal alloy oxidizes and returns to a low-energy state similar to that of metal ore. Differences in the crystal structure of pieces of metal set up a voltaic cell. This can occur within a single sheet of metal, or between two sheets that are in contact with each other [15].

Electrochemically, corrosion is the transport of ions from the anode to the cathode, in the process of freeing metal atoms that can subsequently bind with oxygen (Fig I. 1). For corrosion to function, there need to be one or more metals, an electrolyte (salts in solution), and oxygen. The corrosion product of iron (Fe2O3), however, hydrates easily and thereby continually flakes off to expose a fresh metal surface [15].

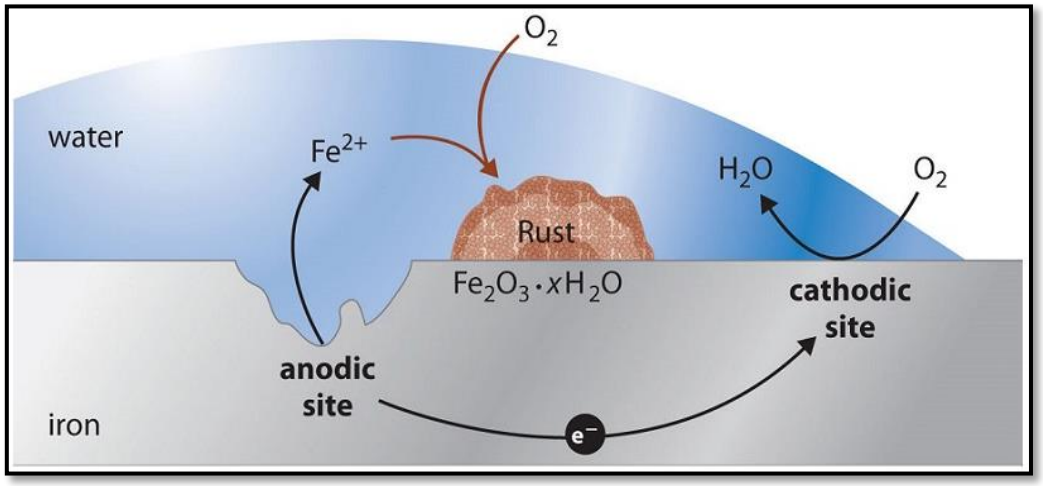

Figure I. 1: Basic corrosion process [16].

$$Fe \rightarrow Fe^{+2}(aq) + 2e^{-} \quad \text{Equ I. 1}$$

$$O_2(g) + 2H_2O(l) + 4e^{-} \rightarrow 4OH^{-}(aq) \quad \text{Equ I. 2}$$

$$Fe^{+2}(aq) + 2OH^{-}(aq) \rightarrow Fe(OH)_2(s) \quad \text{Equ I. 3}$$

$$Fe(OH)_2(s) + O_2(g) \rightarrow 2Fe_2O_3.xH_2O \quad \text{Equ I. 4}$$

At the anode, solid iron is oxidized to $Fe_2^{+}$and enters the electrolytic solution. The two freed, negatively charged electrons (e^{-}) are transferred from the anode to the cathode through the electrically conductive metal(s). At the cathode. Oxygen from the air is reduced to hydroxide ions (OH^{-}). The Fe_2^{+} in the electrolytic solution reacts with the hydroxide ions to precipitate Fe $(OH)_2$ which oxidizes with atmospheric oxygen, forming red-brown hydrated ion oxide ($Fe_2O_3 \cdot xH_2O$) [15].

I.1.2 standard hydrogen electrode (SHE)

The standard hydrogen electrode (abbreviated SHE), is an oxidation-reduction (redox) electrode which forms the basis of the thermodynamic scale of oxidation-reduction potentials. Its absolute electrode potential is estimated to be 4.44 ± 0.02 V at 25 °C, but to form a basis for comparison with all other electro-reactions, hydrogen's standard electrode potential (E°) is declared to be zero volts at any temperature.

Table I. 1: standard hydrogen electrode (SHE) [17].

Reaction	E° (V vs. SHE*)
$Au \rightarrow Au^{3+} + 3e^-$	+1.498
$2H_2O \rightarrow O_2 + 4H^+ + 4e^-$	+1.229
$Ag \rightarrow Ag^+ + e^-$	+0.799
$4OH^- \rightarrow O_2 + 2H_2O + 4e^-$	+0.40
$Cu \rightarrow Cu^{2+} + 2e^-$	+0.34
$H_2 \rightarrow 2H^+ + 2e^-$	0.00
$Pb \rightarrow Pb^{2+} + 2e^-$	–0.126
$Ni \rightarrow Ni^{2+} + 2e^-$	–0.257
$Co \rightarrow Co^{2+} + 2e$	–0.280
$Fe \rightarrow Fe^{2+} + 2e^-$	–0.447
$Cr \rightarrow Cr^{3+} + 3e^-$	–0.744
$Zn \rightarrow Zn^{2+} + 2e^-$	–0.762
$Ti \rightarrow Ti^{2+} + 2e^-$	–1.63
$Al \rightarrow Al^{3+} + 3e^-$	–1.67
$Mg \rightarrow Mg^{2+} + 2e^-$	–2.37

I.1.3 Corrosion of carbon steel

In the petroleum industry, carbon steel is the most commonly used material in piping, both upstream and downstream. As such, carbon steel is an important material due to its good mechanical performance and relatively low cost compared to higher alloy materials [18]. In addition, the corrosion resistance of these materials is poor, meaning that engineering products have a shorter lifetime and less performance. Therefore, methodologies are required that inhibit corrosion [19].

I.1.4 Oxidizing Agents

the two main oxidizing agents encountered in practice are [20]:

- Solvated protons (H^+)
- Dissolved oxygen (O_2)

However, other oxidants can also corrode metals, such as [20]:

- Oxidizing metal cations: $Cu2^+$, $Fe2^+$, $Fe3^+$ $Sn4^+$
- oxidizing anions: NO-2, NO-3, CrO2-4.-, MnO-4, OCl-
- dissolved oxidizing gases: O3, C12, SO3

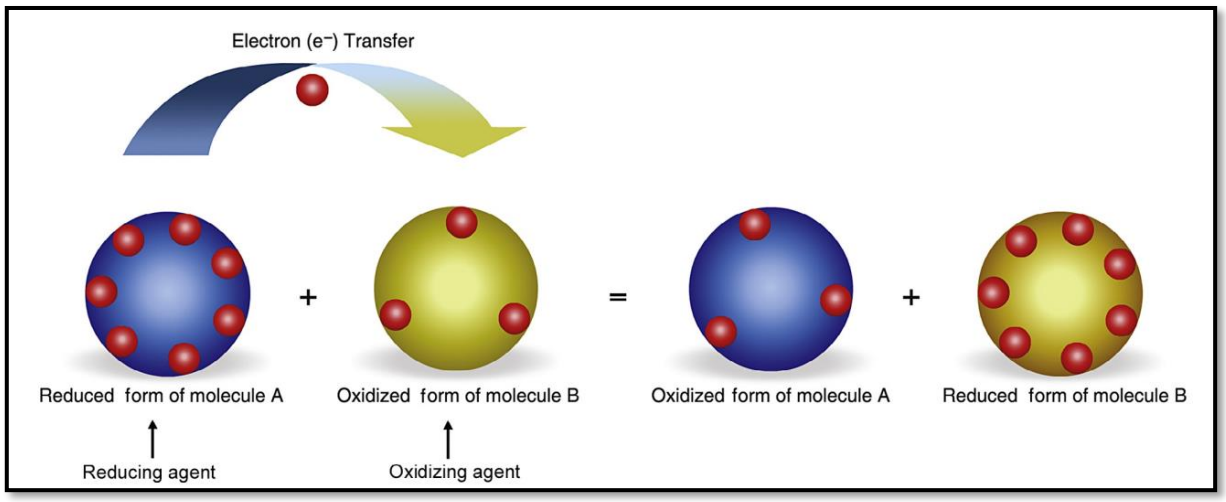

Figure I. 2: A full oxidation-reduction reaction involves the transfer of electrons from one species (the reducing agent) to another (the oxidizing agent) [21].

I.1.5 Types of corrosion of carbon steel (API 5L X70)

I.1.5.1 Sour corrosion

Sour corrosion is a customary term for aqueous corrosion in the presence of hydrogen sulfide (H_2S) at a level high enough to significantly affect the corrosion behavior and corrosion products compared with otherwise the same conditions without H_2S. Sour corrosion may take place on all upstream and downstream steel components exposed to H_2S, such as well tubing, flowlines, transport pipelines, and processing equipment. illustrates a cross-section of an example of a multiphase wet gas pipeline with the different liquid and gaseous phases indicated [22].

The general mechanism of H_2S corrosion involves the gradual desorption of metallic Fe, the formation of FeS (mackinawite) in the anodic region, and the simultaneous reduction of H+ ions to H_2 in the cathodic region (Fig. 04) [23].

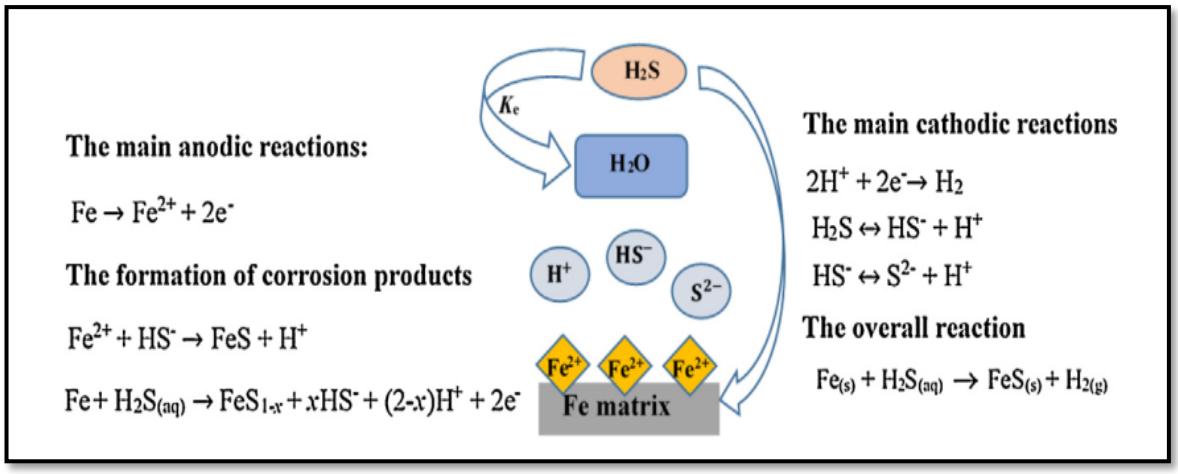

Figure I. 3: General mechanism of iron oxidation in an H2S environment [23].

I.1.5.2 Under Deposit Corrosion

The under-deposit mechanism can increase the corrosion reaction rate by causing a localized chemical concentration which results in the pitting of the metal surface under solid deposits. These deposits appear to be composed of a corrosion product matrix with entrapment of formation solids, sand, and iron sulphide. The rate of corrosion under this mechanism is significantly lower than an erosion-corrosion mechanism [24].

I.1.5.3 Sweet corrosion (CO_2 corrosion)

CO_2 corrosion or sweet corrosion has been a recognized problem in oil and gas production and transportation facilities for many years. CO2 is one of the main corroding agents in oil and gas production systems. Dry CO2 gas is not itself corrosive at the temperatures encountered within oil and gas production systems but is so when dissolved in an aqueous phase through which it can promote an electrochemical reaction between steel and the contacting aqueous phase. CO2 will mix with the water, forming carbonic acid making the fluid acidic and is by far the most prevalent form of attack encountered in oil and gas production. At elevated temperatures, an iron carbide scale is formed on the oil and gas pipe as a protective scale, and the metal starts to corrode under these conditions [25] (Fig. 05).

Main reaction [26]: $Fe + CO_2 + H_2O = FeCO_3 + H_2$ Equ I. 5

Figure I. 4: Sweet corrosion (CO2 corrosion) [27].

I.1.5.4 Microbiologically induced corrosion

This type of corrosion is caused by bacterial activities. The bacteria produce waste products like CO2, H2S, and organic acids that corrode the pipes by increasing the toxicity of the flowing fluid in the pipeline. The microbes tend to form colonies in a hospitable environment and allow enhanced corrosion under the colony. The formation of these colonies is promoted by neutral water especially when stagnant [28].

Figure I. 5: Microbial corrosion inside pipeline [29].

I.1.5.5 Crevice Corrosion

Crevice corrosion results when a portion of a metal surface is shielded in such a way that the shielded portion has limited access to the surrounding environment. Such surrounding environment contain, damaging corrosion species usually chloride ions. A typical example of crevice corrosion is the crevice found at the area between two metal surfaces in close contact with a gasket or another metal surface. The environment that eventually forms in the crevice is similar to that formed under the precipitated corrosion that covers a pit. An electrochemical corrosion cell is formed from the couple between the unshielded surface and the crevice interior exposed to an environment with a lower oxygen concentration compared with the surrounding medium. The concentration of being the anode of a corrosion cell and existing in an acidic, high-chloride environment where repassivation is difficult makes the crevice interior subject of corrosion attack [24].

Figure I. 6: Oil and gas pipeline under crevice corrosion [28].

I.1.5.6 Erosion-Corrosion

The erosion-corrosion mechanism increases the corrosion reaction rate by continuously removing the passive layer of corrosion products from the wall of the pipe. The passive layer is a thin film of corrosion product that actually serves to stabilize the corrosion reaction and slow it down. As a result of the turbulence and high shear stress in the line, this passive layer can be removed causing the corrosion rate to increase. The erosion-corrosion is always experienced where there is high turbulence flow regime with a significantly higher rate of corrosion than just corrosion or erosion in the pipeline. In a multiphase flow regime with a fully developed turbulent flow, bubbles development and collapse have been attributed to changes in mass transfer coefficient and an eventual increase in CO2 corrosion [24].

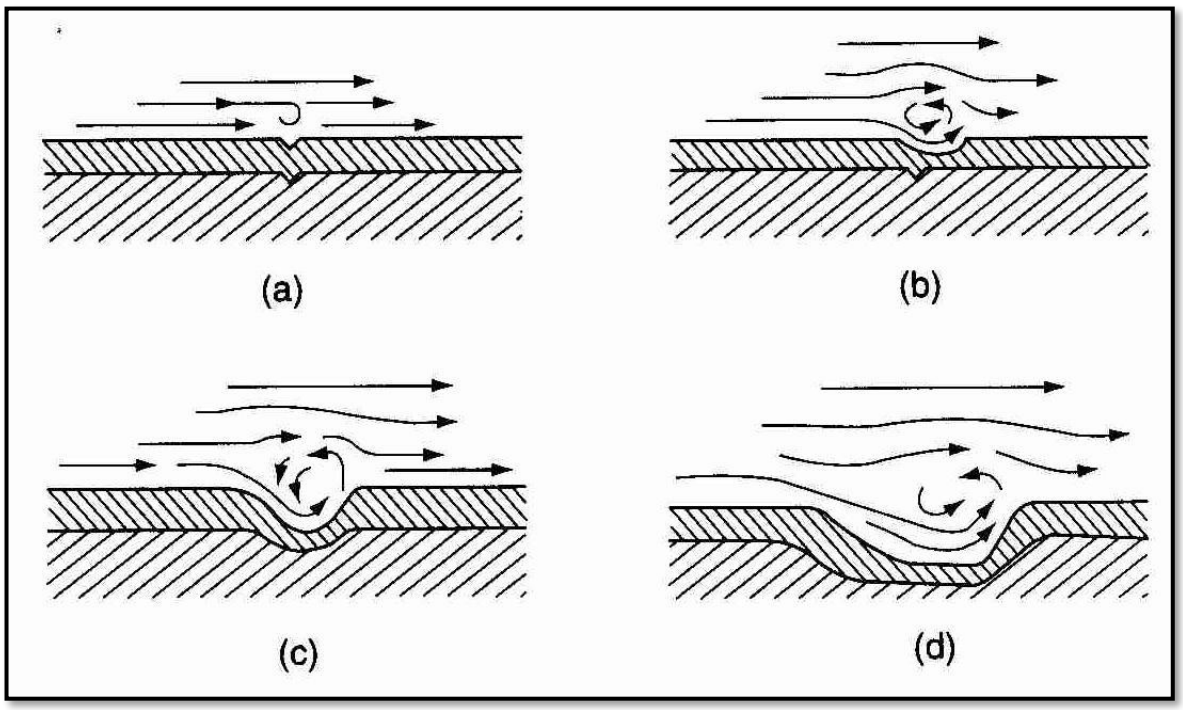

Figure I. 7**:** Erosion corrosion process [30].

I.1.6 Corrosion mechanism in acidic media

The corrosion rate is higher in an acidic environment in which hydrogen gas is liberated through a cathodic reaction. Hydrogen ejected from the metallic surface either reunite and leave as gas or enter into metal producing the hydrogenï activated deterioration of the metal [31]. The figure I-08 shows the corrosion process.

Main Reactions [32]:

Anodic Reaction (Oxidation):

$Fe \rightarrow Fe^{+2}(aq) + 2e^{-}$ Equ I. 6

Cathodic Reaction (Reduction):

$2H^{+} + 2e^{-} \rightarrow H_2$ Equ I. 7

Global Reaction (Oxidation /Reduction):

$Fe + 2H^{+} \rightarrow Fe^{+2} + H_2$ Equ I. 8

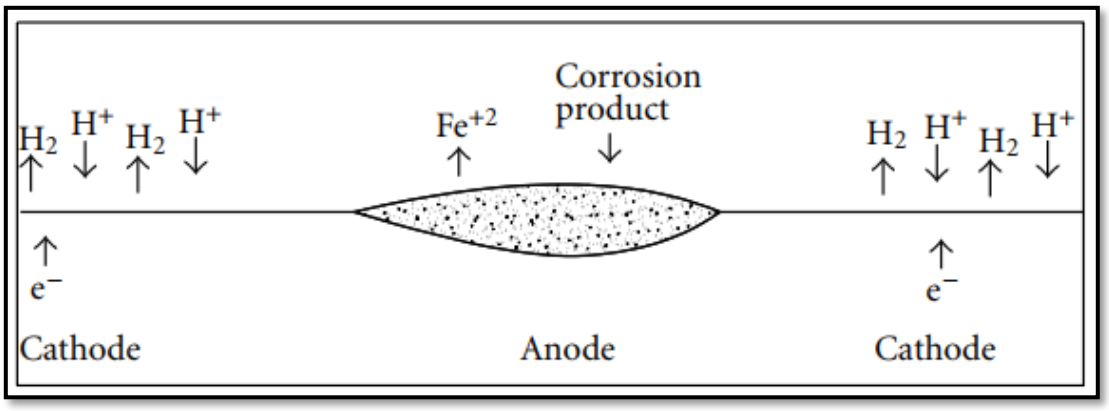

Figure I. 8: Corrosion Process in acidic media [29].

I.1.7 Acids solutions

Aqueous solutions of acids are among the most corrosive media. Some important fields of acid applications are acid pickling, industrial cleaning, rust and scale removal, oil well acidification in oil recovery, and the petrochemical processes. Hydrochloric and sulfuric acids are the most widely used chemicals to remove undesired scales, such as the rust or mill scale formed during industries of steel and iron-based alloys. However, these two acids are highly aggressive causing severe corrosion problems [33]. Petrochemical industry corrosion can be found in three different areas [34]:

- Production
- Transportation and Storage
- Refinery operations

I.1.8 Oil well stimulation (Acid Injection)

I.1.8.1 Acid Injection (Acidizing)

Acidizing is the process of injecting acid into a damaged wellbore or other damaged formation that can yield oil and gas. This operation is intended to improve the well's productivity or injectivity [35] t h r o u g h t h e a c i d ô s a b i l i t y t o [36].

Damaged wells are those which suffer a restriction in flow rate. This may be due to a number of causes, for example, drilling damage or build-up of carbonate scale. Damage may occur at the wellbore face or as a zone of reduced permeability extending several inches or even feet into the formation which severely restricts productivity. If the damage can be removed, very significant increases in production rate can be achieved [37]. There are three general categories of acid treatments:

A- In acid washing: the objective is simply tubular and wellbore cleaning. Treatment of the formation is not intended. Acid washing is most commonly performed with hydrochloric acid (HCl) mixtures to clean out the scale (such as calcium carbonate), rust, and other debris restricting flow in the well [38].

B- Matrix acidizing: The process involves the injection of acid mixtures below the fracture pressures of rocks near the wellbore. Its purpose is dissolving sediments to reinforce rock permeability and the establishment of a clean zone within the reservoir, thus eliminating the restrictions for oil flux into the wellbore zone. Commonly, matrix acidizing is applied in case of tighter carbonate and sandstone formations, it is recommended in the industry to utilize acids with mass concentrations, in the range of 10ï 15% [38].

C- Fracture acidizing: is implemented in case of carbonate formations with relatively higher acid mass concentrations, in the range of 20ï 30%. This method involves acid injection above the fracture pressures of rocks near the wellbore to create channels or so-called wormholes, as the resulting rock fractures, under pressure from the hydrocarbons, might immigrate through [38].

I.1.8.2 The main Stages of acidizing

A- Pre-flush stage is employed to dissolve any Na, K, and Ca ions that may produce insoluble silicates when reacted with the silica. Besides preventing the live HF acid to enter into a high pH region, pre-flush also provides a low pH region reducing the risk of precipitate formation [39].

B- Main acid stage is applied to dissolve the quartz, clay, feldspar and silicates. This acid may also dissolve the remains of carbonates present after the pre-flush stage [39].

C- After-flush stage is used to keep the wettability of the formation to the original state and it cleans the formation rapidly by removing the spent acid. Mutual solvents, diesel oil, NH_4Cl, acetic acid, or HCl can be applied at this stage for the efficient displacement of the spent acids [39].

I.1.8.3 Conventional acid systems

A number of different acids are used in conventional acidizing treatments, the most common are [37]:

Hydrochloric, HCl

Hydrofluoric, HF

Acetic, CH_3COOH

Formic, HCOOH

Sulfamic, H_2NSO_3H

Chloroacetic, $ClCH_2COOH$

These acids differ in their characteristics. Choice of the acid and any additives for a given situation depends on the underground reservoir characteristics and the specific intention of the treatment, for example near wellbore damage removal, dissolution of scale in fractures, etc. The majority of acidizing treatments carried out utilize hydrochloric acid (HCl). However, the very fast reaction rate of hydrochloric acid, and other acids listed above, can limit their effectiveness in a number of applications. All conventional acids including HCl and organic acids react very rapidly on contact with acid-sensitive material in the wellbore or formation. Worm holing is a common phenomenon. The rapid reaction means the acid does not penetrate very far into the formation before it is spent. Conventional acid systems are therefore of limited

effectiveness in treatments where deep acid penetration is needed. Problems in placing acid are compounded in long horizontal or directional wells. In these wells, it is difficult to achieve truly uniform placement of acid along the well-bore, which may be several thousand meters long, let alone achieve uniform stimulation of the surrounding formation [37].

I.1.8.4 Formation Type and Reaction with Acids

I.1.8.4.1 Sandstone Formations

The purpose of sandstone matrix acidizing is the removal of siliceous particles such as formation clay, feldspar, and quartz fines that are restricting near-wellbore permeability, plugging perforations, or gravel packs. This is accomplished with the injection of acid formulations containing hydrofluoric (HF) acid or its precursors, as HF is the only common acid that dissolves siliceous particles sufficiently. Such plugging particles may be naturally occurring or may have been introduced into the formation during well operations [40].

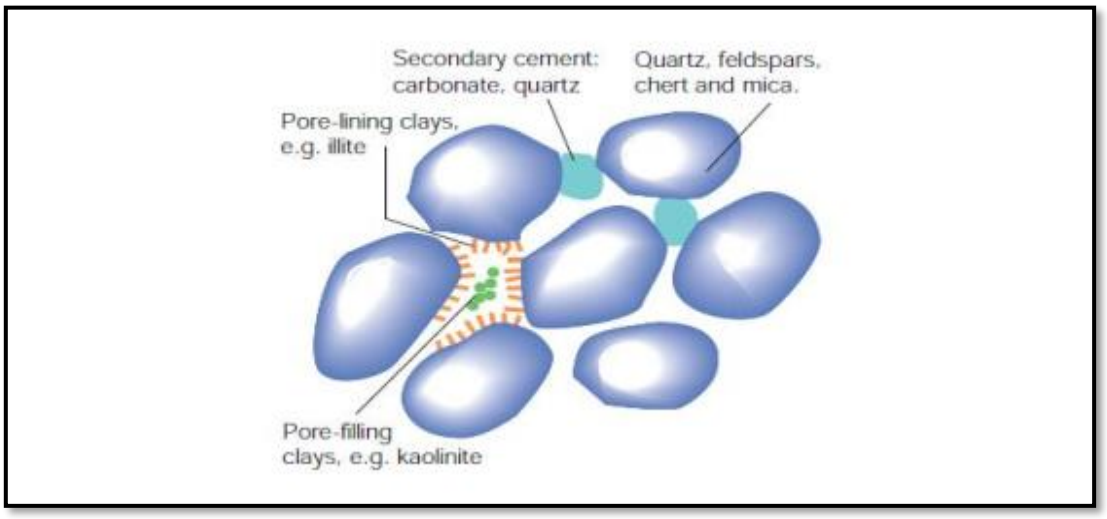

Figure I. 9**:** Constituents of Sandston [41].

I.1.8.4.2 Carbonate Formations

The objective when acidizing carbonate formations is to dissolve carbonate-based materials to create new or clean existing pathways or channels that allow the formation fluids (oil, gas, and water) to flow more freely into the well [41].

Acid dissolution of carbonates reactions [42]:

$CaCO_3 + H_2SO_4 \rightarrow CaSO_4 + CO_2 + H_2O$ Equ I. 9

$CaMg(CO_3)_2 + 2H_2SO_4 \rightarrow MgSO_4 + CaSO_4 + 2CO_2 + 2H_2O$ Equ I. 10

I.2 Protection of carbon steel against corrosion in acidic media by corrosion Inhibitors

Among the methods to avoid or prevent the destruction or degradation of metal surfaces, the corrosion inhibitors are one of the best know methods of corrosion protection and one of the most useful in the industry. this method is following stand up due to its low cost and practice method [43].

I.2.1 Inhibitor

An inhibitor is a substance (or a combination of substances) added in a very low concentration to treat the surface of a metal that is exposed to a corrosive environment [44], to prevent or minimize the corrosion process [43]. These are also known as site blocking elements, blocking species, or adsorption site blockers, due to their adsorptive properties [44]. Inhibitors slow corrosion processes by [45]:

¶ Reducing the anodic and cathodic reaction speed

¶ Reducing the movement or diffusion of ions from the metallic surface

¶ Increasing the electrical resistance of the metal surface

Corrosion inhibitors play a vital role to reduce hydrogen evolution by adsorption phenomenon that subsequently inhibits corrosion and protects the metal surface [31].

The effectiveness of inhibitors depends on [31]:

- ¶ Solution corrosives
- ¶ Concentration
- ¶ Temperature
- ¶ pH
- ¶ Dissolved salts

I.2.1.1 Inorganic inhibitors

Inorganic inhibitors such as dichromates, chromates, tungstates, molybdates, nitrites, and nitrates have been used as corrosion inhibitors. These inhibitors are powerful oxidizing agents. They have other important roles such as chelating agent and abrasive particle. The effectiveness of some corrosion inhibitors depends upon the type of material, its properties and the corrosion environment. For instance, inhibition efficiency of molybdate anion increases with the increasing of oxygen concentration in a corrosion environment. Some of these anions have been used satisfactorily in many corrosive environments. For example, molybdates have been used to prevent mild steel corrosion, on bacterial corrosion. Nitrates have been used to prevent galvanized steel, and zinc corrosion in NaCl solution. Chromates are a very effective corrosion inhibitors for iron and ferrous alloys in the presence of halide ions [46].

I.2.1.2 Organic inhibitors

Organic corrosion inhibitors are a class of molecules that delay or minimize the corrosive process. It has been shown that their effectiveness is mainly related to adsorption on the metal surface, acting as a barrier layer and reducing aggressive species access, usually, they get adsorbed on the metal surface by displacing water molecules, and the bonding efficiency is enhanced by the presence of polar functions with S, O, or N atoms in the molecule, heterocyclic compounds, and electrons [19].

I.2.1.3 Synthetic Organic Corrosion Inhibitors

The use of synthetic corrosion inhibitors is the most popular and effective method due to their association with cost-effective synthesis, high effectiveness and ease of application. The effectiveness of these organic inhibitors is based on the fact that generally they contain several heteroatoms in the form of polar functional groups such as ï OH, -NO2, -OCH3, - COOH, -NH2, - COOC2H5, -CONH2, etc [47].

I.2.2 Inhibition Mechanism of organic inhibitors

When metals come in close contact with aggressive media, their surfaces corrode. The speed and extent of the corrosion process depends on several factors like concentration of the aggressive medium and temperature. Corrosion inhibitors have been employed extensively to control corrosion of metals in various aggressive media. It is generally believed that a given corrosion inhibitor functions by adsorption on metal surface and formation of thin protective film(s) or layer(s) that óblanket(s)ô the me

of interaction between the film formed and the metal surface may be explained with the help of adsorption isotherms. Adsorption involves adhesion (or concentration) of atoms, molecules or ions on the surface of a substance, most often, a solid. The surface to which the molecule or atom is adhering is called the adsorbent while the molecule or atom itself is called the adsorbate. Therefore, the adsorption phenomenon is essentially an attraction of adsorbate species on the adsorbent surface. The preferential concentration of adsorbate molecules in the proximity of the adsorbent surface arises from the unsaturated nature of surface forces of the adsorbent. Verma et al. opines that adsorption of corrosion inhibitors may be seen as a substitution process where the inhibitor molecules in the aqueous phase replace water molecules already adsorbed on metal surface. The mechanism by which adsorption takes place may be physical or chemical in nature, also referred to as physisorption or chemisorption respectively [48].

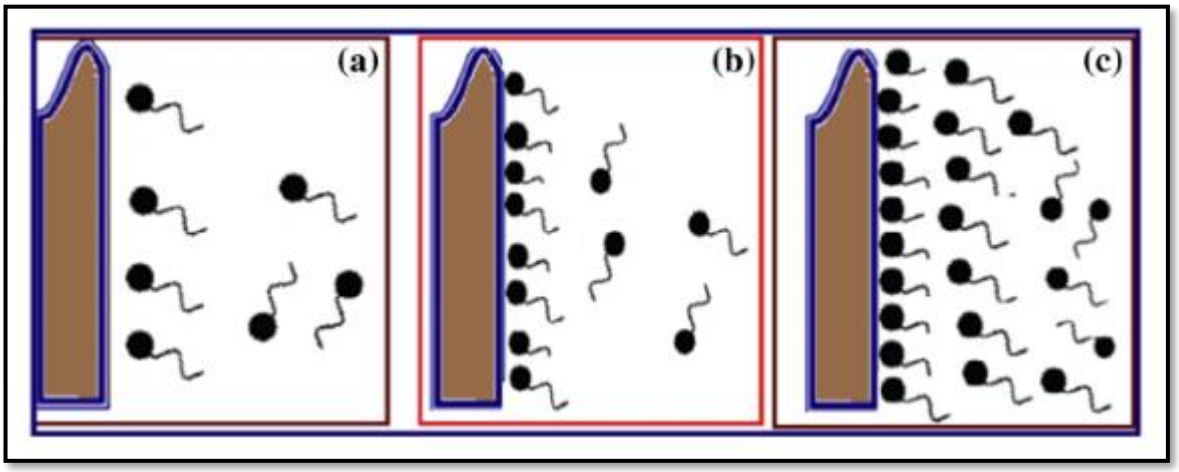

Figure I. 10**:** Inhibitor adsorption on mild steel surface. (a) Adsorption in the presence of inhibitor at a low concentration. (b) Adsorption in the presence of inhibitor at a high concentration. (c) Adsorption in the presence of inhibitor at a higher concentration [49].

I.2.2.1 Physical Adsorption

As result of the bonds that those atoms have with the neighboring atoms of the same substance. Adsorption is carried out on such surfaces through natural attractive forces or the so-called vander waals forces. This type of adsorption can be in the form of multiple layers of the adsorbent material on the surface of the adsorbent material when suitable conditions of pressure and temperature are available. The adsorbent and the adsorbent, which is estimated at less than (40 kj/mol), therefore, this type of adsorption does not need high temperatures and

does not require activation energy and occurs at low temperatures similar to the process of condensation of vapors on the surfaces of liquid materials [50].

I.2.2.2 Chemical Adsorption

This type of adsorption occurs on surfaces that are not electronically unsaturated, as such surfaces tend to form chemical bonds with the atoms or molecules that have been adsorbed. As a first step in the chemical reaction that occurs between the adsorbent surface and the adsorbent material, this type of adsorption needs a high activation energy, as well as the accompanying temperatures are high and estimated in a quantity greater than (40 kj/mol), and this type of adsorption is specific and is not reversed and limited by its layer Oxygen adsorption on coal surface, hydrogen chloride adsorption on iron surface. The Factors affecting on Adsorption [50].

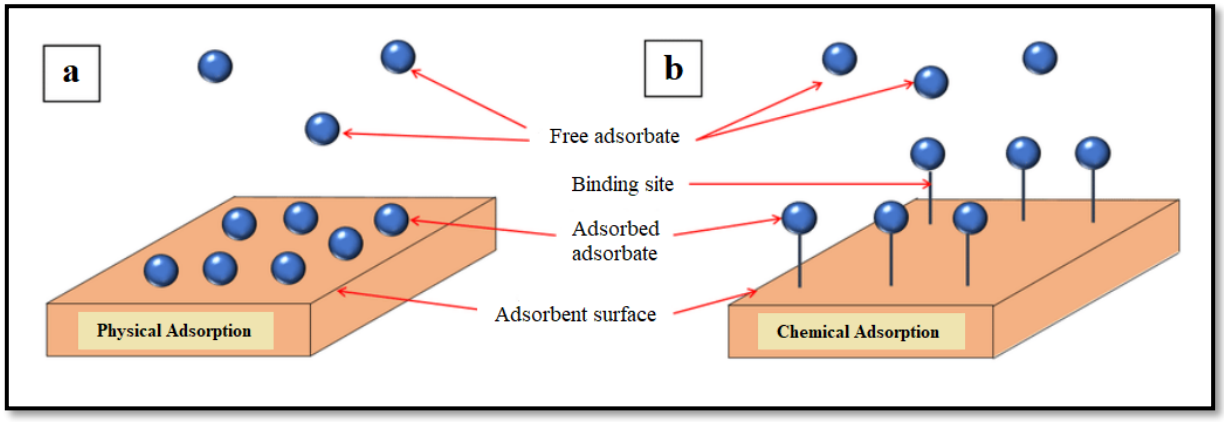

Figure I. 11**:** The mechanism of (a) Physical and (b) Chemical adsorption [51].

I.2.3 Problems of cost and toxicity of inhibitors

These organic inhibitors are effective against corrosion, but at the same time the processing time, cost, and toxic nature have compelled researchers to look for alternatives. The inhibiting effect of some of these organic compounds on the corrosion of mild steel has been recently reported by several authors. However, most of the compounds that constitute these inhibitors are expensive and toxic to humans and the environment. The toxicity of these organic inhibitors led to exploring the use of nontoxic, biodegradable, and eco-friendly. [52].

I.3 Eco-friendly inhibitors for carbon steel in acidic media

The term ñgreen-friendly inhibitorsò refers to biocompatibility in nature. The inhibitors like plant extracts presumably possess biocompatibility due to their biological origin. Similar to the general classification of ñinhibitorsò, ñgreen inhibitorsò can also be inhibitors and inorganic green inhibitors [44].

I.3.1 Natural polymers as corrosion inhibitors in acidic media for carbon steel

The use of polymers as corrosion inhibitors has attracted considerable attention recently. Polymers are used as corrosion inhibitors because, through their functional groups they form complexes with metal ions and on the metal surface these complexes occupy a large surface area, thereby blanketing the surface and protecting the metal from corrosive agents present in the solution. The inhibitive power of these polymers is related structurally to the cyclic rings, heteroatom (oxygen and nitrogen) that are the major active centers of adsorption. Polymers found in nature have shown promising results as metal corrosion inhibitors in different corrosive environments [41].

I.3.2 Aloe Vera

Aloe vera is a genus of shrubby succulent plants in the lily family (liliaceae). It is a very shortï stemmed succulent plant growing to 80ï 100 cm tall, spreading by offsets and root sprouts. The leaves are lanceolate, thick and fleshy, green to greyï green, with a serrated margin [53].

Generally speaking, aloes are leaf-succulent plants with simple leaves. They often have teeth along the margins although some species also have prickles or teeth on the leaf surface. Leaves are often rosulate (acaulescent) or distributed along the stem. The caulescent species might still have a rosulate distribution of the leaves, with a rosette at the end of the trunk [50].

Figure I. 12: Aloe Vera [54].

Aloe plant extract is organic in nature and can be used in the production of green inhibitors, and it is one of natural inhibitors which has an inhibitive action on the corrosion of metals. Aloe Vera gel (AVG) is the colorless mucilaginous gel obtained from the parenchymaous cell in the fresh leaves of Aloe Vera. It contains various active compounds such as salicylates, magnesium lactate, acemennan, lupeol, campestrol, sterol, linolenic, aloctin and anthraquinones [56].

Figure I. 13: Inside Aloe Vera leaf [54].

I.3.3 Chemical composition and molecular structure of Aloe Vera

There are more than two hundred different types of chemical compounds in aloe vera. The aloe vera leaf gel contains about 98 to 99% water. The total solid content of the extracted gel is about 0.66% and soluble solids are 0.56%. On dry matter basis extracted gel consists of polysaccharides 55 %, sugars 17 %, minerals 16 %, proteins 7 %, lipids 4 % and phenols 1 %. The major polysaccharide is acemannan, the A. Vera gel contains several important vitamins such as vitamins E, C and A. Vitamin B1 (thiamine), niacin, Vitamin B2 (riboflavin), choline, and folic acid are also presented in figure [56].

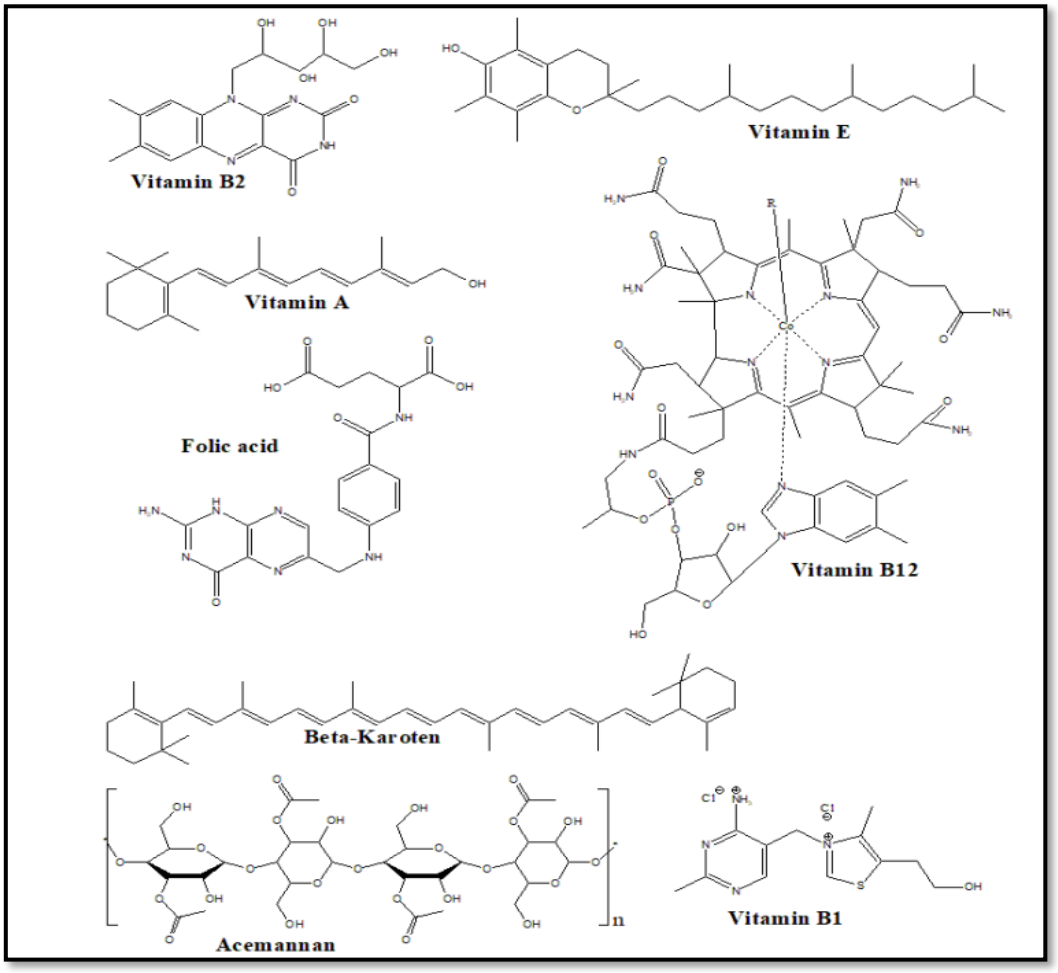

Figure I. 14: Major components of Aloe Vera gel [56].

Chapter II : Experimental Techniques

An overview of electrochemical and surface analysis as methods for this study will be discussed in this chapter, along with information about experimental parts.

II.1 Techniques of studies

In order to investigate corrosion and inhibitor efficiency in a corrosive medium such as sulfuric acid (H_2SO_4), in this study, two methods been applied:

- **Electrochemical methods**: The purpose of this test is to determine the inhibition efficiency and mechanism of a selected inhibitor in corrosive medium (H_2SO_4).

- **Surface analysis:** used to characterize the corrosion process by analysing the state of the sample surface, and from there to evaluate the inhibition efficiency.

II.1.1 Electrochemical Methods

Electrochemical methods include Electrochemical impedance spectroscopy (EIS) and potentiodynamic polarization are analytical techniques that use a measurement of potential, charge, or current to determine an analyte's concentration or to characterize an analyte's chemical reactivity. These techniques are used to control and measure the oxidation and reduction reaction rates.

II.1.1.1 Electrochemical Impedance spectroscopy (EIS)

Electrochemical impedance spectroscopy is a powerful technique for characterizing a wide variety of electrochemical systems and for determining the contribution of electrode or electrolytic processes in these systems [57].

The EIS technique works in the frequency domain and is based on the concept that an interface can be seen as a combination of passive electrical circuit elements, **resistance**, **capacitance**, and **inductance** (Figure II.1). When an alternating current is applied to these elements, the resulting [57]. Table II-1 lists the common combined circuit elements, the equation for their current versus voltage relationship, and their impedance [41].

Table II. 1: Common Electrical Elements [41].

Component	Current Vs. Voltage	Impedance
resistor	E= IR	Z = R
inductor	E = L di/dt	Z = jωL
capacitor	I = C dE/dt	Z = 1/jωC

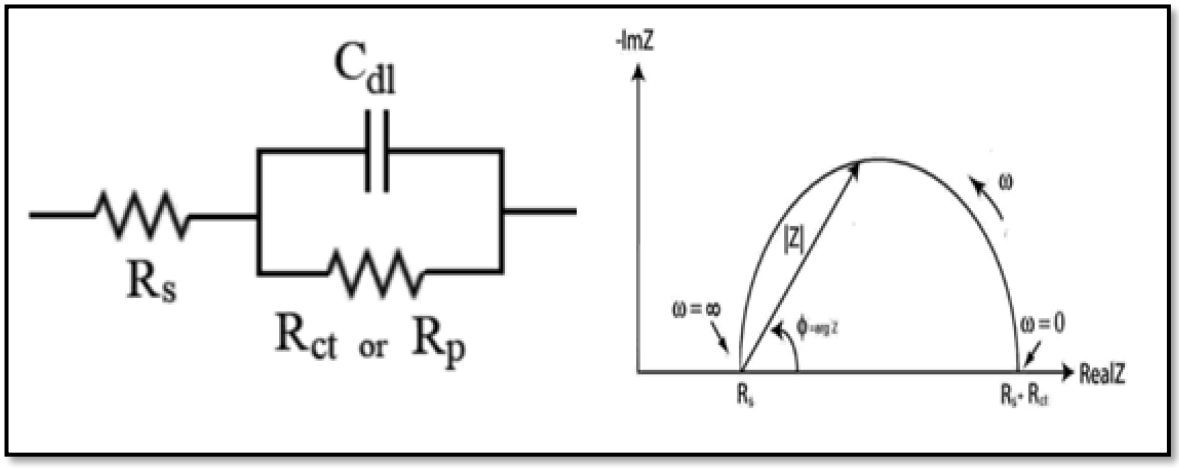

Figure II. 1: Circuit comprising the resistance of the Rs solution, in series with the assembly [58].

The following figures are an examples illustrates the Bode and Nyquist plots curves for Mild Steel samples exposed to 0.5M H_2SO_4 Solution and with different concentrations of *Myristica fragrance* (MF) extract.

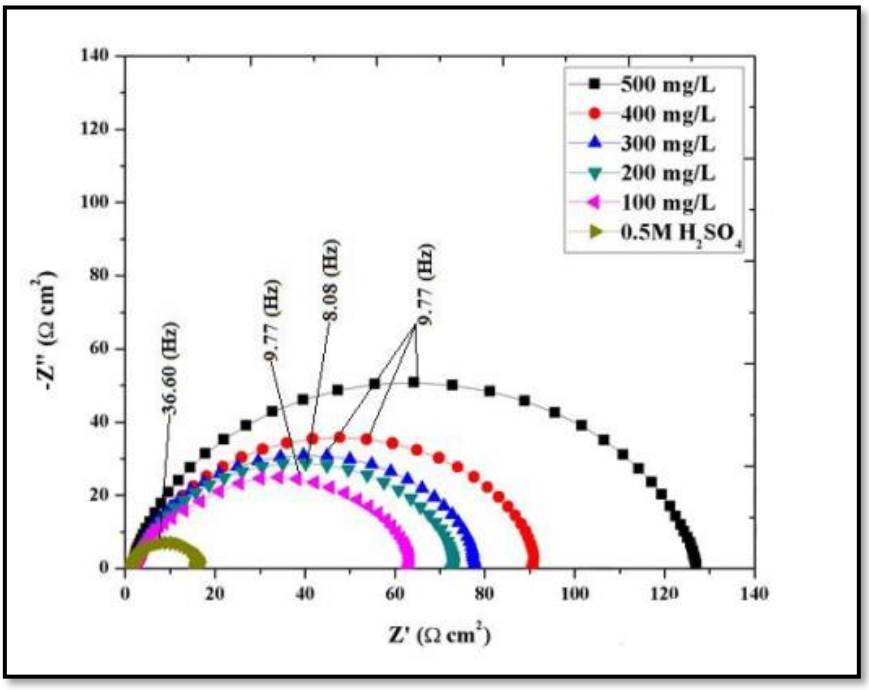

Figure II. 2: Nyquist plots curves for mild steel sample immersed in 0.5M H_2SO_4 solution with 0-500 mg/L concentrations of *Myristica fragrance* extract [59].

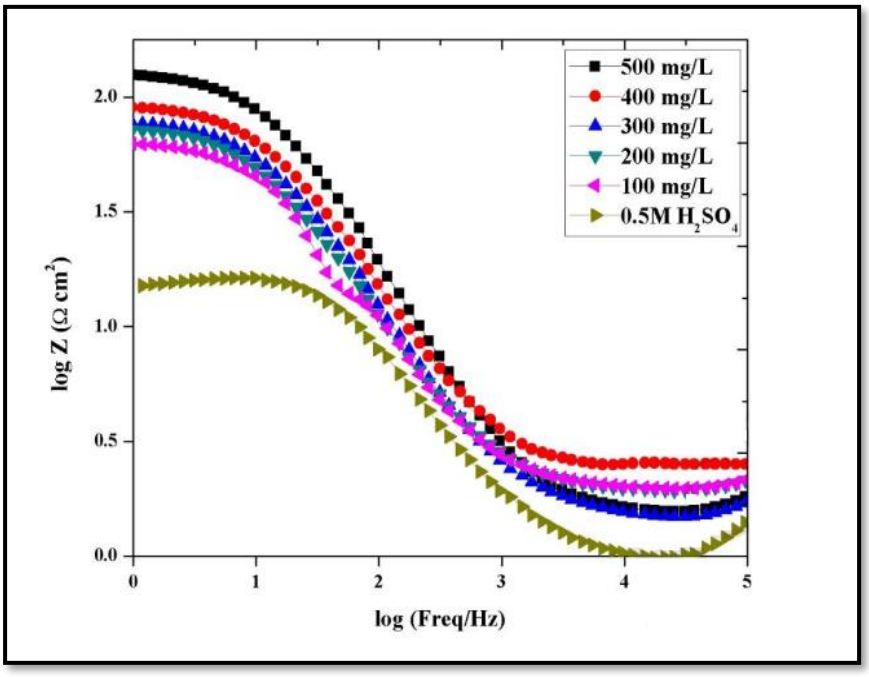

Figure II. 3: Bode-Z plots curves for mild steel sample immersed in 0.5M H_2SO_4 solution with 0-500 mg/L concentrations of *Myristica fragrance* extract [59].

II.1.1.2 Potentiodynamic polarization

The potentiodynamic polarization investigation can be used to determine the chemical behavior of the sample performance. The analysis from the evaluation can provide substantial experimental data about the material degradation mechanisms, decay rate, and performance. the potentiodynamic polarization analysis can provide specific detailed information about the corrosion rate and corrosion potential of a given sample [60].

A conventional potentiodynamic polarization analysis includes a three-electrode system arrangement of a counter electrode, a reference electrode, and a sample as the working electrode. The performance of the electrodes in a potentiodynamic polarization examination depends on the largest possible region ascertained by potentiodynamic sweeping, which sweeps in a range of potentials from the passive to the active region on the potentiodynamic curve. The potentiodynamic polarization provides exhaustive information about the anodic charge, open circuit, rupture, and passivation potential. It also provides information about the passive range and sensitivity to pitting corrosion [60]. Figure II.4 represent logarithmic Potentiodynamic polarization curve of corrosion rate.

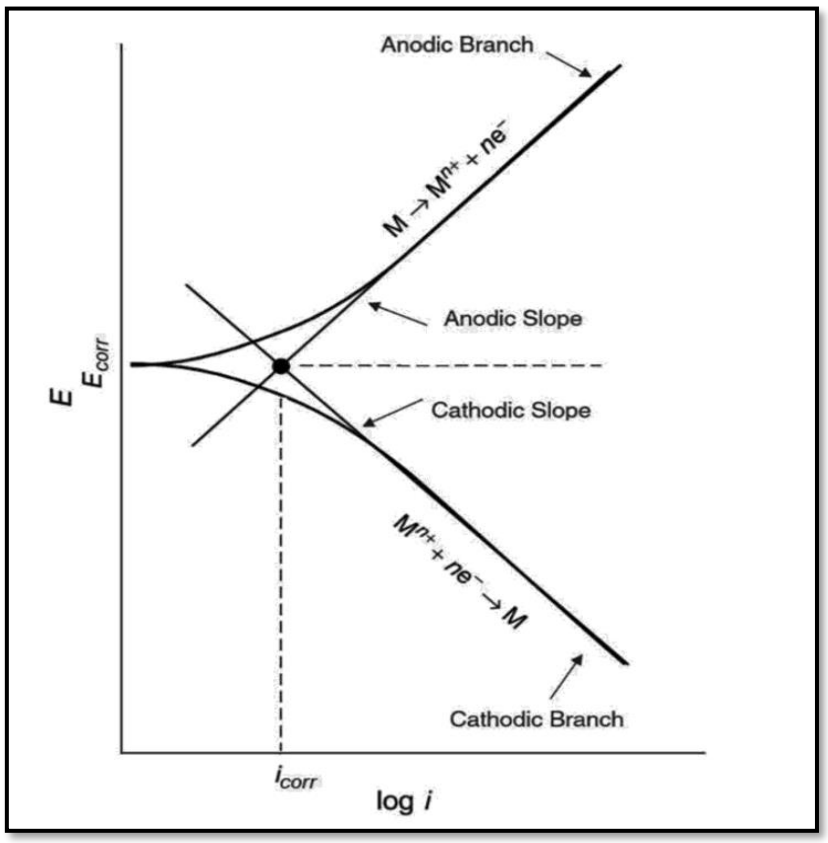

Figure II. 4: Corrosion rate [58].

II.1.2 Surface analysis

An Optical Microscope (OM) is used to provide clear images and information of the surface sample [61], specifically with regard to the morphology and corrosion type [62].

II.2 Experimental Conditions

II.2.1 Material (working electrode)

The working electrodes (API 5L X70 pipeline steel), for electrochemical experiments, were cut into 3 × 3 × 1 cm^3. The chemical composition of API 5L X70 pipeline is showing in table II-2.

- *API (The American Petroleum Institute)* 5L means: Is a carbon steel pipe used in oil and gas transmission systems. Additionally, API 5L can also be applied to other fluids, such as steam, water, and slurry, for transmission purposes.

- X70 means: Steel grade (example: A25, A, B, X42, X52, X56, X60, X65, X70, X80).

- The number 70 means: 70 000 psi, elastic limit in psi (pound per square inch).

Table II. 2: Chemical composition of API 5L X70 (weight percentage)

C (Max)	Mn (Max)	Si (Max)	P (Max)	S (Max)	Cr (Max)	Ni (Max)	Nb (Max)	Ti (Max)	Fe
0.12	1.68	0.27	0.012	0.05	0.051	0.04	0.003	0.03	Bal

A 2,85 cm^2 surface area of each electrode was exposed to the electrolyte when the samples were mounted in the electrochemical cell. Using silicon carbide abrasive papers, wet grinding was used to prepare the exposed surfaces of the samples (grade 180, 320, 600, 800, 1000, 1200), following cleaning with distilled water and degreasing with acetone.

II.2.2 Medium (electrolyte)

In this experiment, an aggressive solution of Sulfuric acid was prepared by dilution of 96% H_2SO_4 acid with distilled water was used as an electrolyte.

II.2.3 Inhibitor

An extract gel from Aloe Vera (Figure II.5) was collected and used in May 2022 from Biskra, Algeria, and the inhibition efficiency was tested by putting different concentrations.

Figure II. 5: Aloe Vera plant

II.2.4 Electrochemical Methods

In this investigation, electrochemical impedance spectroscopy (EIS) and potentiodynamic polarization techniques were used to examine the inhibition efficiency of Aloe Vera Gel (AVG) for API 5LX70 in 0.5M Sulfuric acid solution.

Electrochemical measurements were performed using a Gamry Ref 3000 with Gamry Instruments Framework (version 7.05) commercial software.

A Gamry Paracell (Electrochemical Cell) with a standard three-electrode configuration consisting of Ag/AgCl reference electrode (the potential of Ag/AgCl electrode is the same of the saturated calomel electrode and equal to 240 mV vs.NHE), graphite block for Paracell as counter electrode and the sample acted as the working electrode. The working electrode was connected with a copper wire on the backside and installed in customized Teflon assembly and exposed on the solution side to about 2.85 cm^2 working area.

All experiments were performed in stagnant aerated solutions at 30 °C. The working electrode was immersed in test solution at the open circuit potential (OCP) for 1 h to be sufficient to attain a stable state.

The analyses were performed using Gamry Echem Analyst (version 7.05) commercial software developed by Gamry.

II.2.4.1 Potentiodynamic polarization

Potentiodynamic polarization studies were carried out from the cathodic potential of -0.3 V to anodic potential of + 0.3 V with respect to the corrosion potential (E_{corr}) at a scan rate of 0.3 mV/s. The corrosion current densities (I_{corr}) were determined graphically from the cathode part of polarization curve. Similar method has been previously employed for non-Tafel dependence curves with acceptable deviation of less than 10% from other methods of corrosion rate determination.

Because of the presence of a degree of nonlinearity in the Tafel slope part of the obtained polarization curves, the Tafel constants were calculated as a slope of the points after (Ecorr) by ±85 mV.

The values of i_{pd} were calculated using the following equation:

$$\eta_{pd}\% = \frac{I_{corr(in)} - I_{corr(in)}}{I_{corr}} \times 100 \qquad \text{Equ II. 1}$$

Where Icorr and Icorr (inh) represent corrosion current density values without and with inhibitor, respectively.

II.2.4.2 Electrochemical impedance spectroscopy

Inhibitions is calculated on the basis of the equation:

$$\eta ES = \left(\frac{R_t - \acute{R}_t}{R_t}\right) \times 100 \qquad \text{Equ II. 2}$$

Where R_t is charge transfer resistance value without the presence of AVG in acid medium, and R_t is charge transfer resistance value in the presence of AVG.

II.2.5 Surface analysis

The API 5L X70 steel surface was prepared without (blank), with inhibitor, and with inhibitor plus synergy Potassium Iodide (KI); 4 g L-1 AVG was used. After 72 h waiting time, the electrodes were removed from the cells and dried. An OM was used for this study.

Chapter III : Results and Discussion

III.1 Part one: Studying corrosion of API 5L X70 steel in H_2SO_4 medium

In this portion of the report, API 5L X70 steel is investigated in sulfuric acid (H_2SO_4) medium. In order to achieve this, an electrochemical techniques series have been achieved to determine electrochemical parameters, plus the Optical Microscope (OM) was used after corrosion products were removed to examine the corrosion type and the surface damage of steel surface in H_2SO_4 acid medium for surface analyze.

III.1.1 Electrochemical techniques of API 5L X70 steel

III.1.1.1 Potentiodynamic polarization technique

The corrosion rate and several parameters were determined by plotting the anodic and cathodic polarization of a few millivolts around a corrosion potential, with the scanning rate set at 0.3 mV /s, at 30°C and with one hour of immersion.

Figure III-1 represents the linear polarization curves of API 5L X70 steel in 0.5M H_2SO_4 acid media at 30°C.

Figure III-2 represents the logarithmic polarization curves of API 5L X70 steel in 0.5M H_2SO_4 acid media at 30°C.

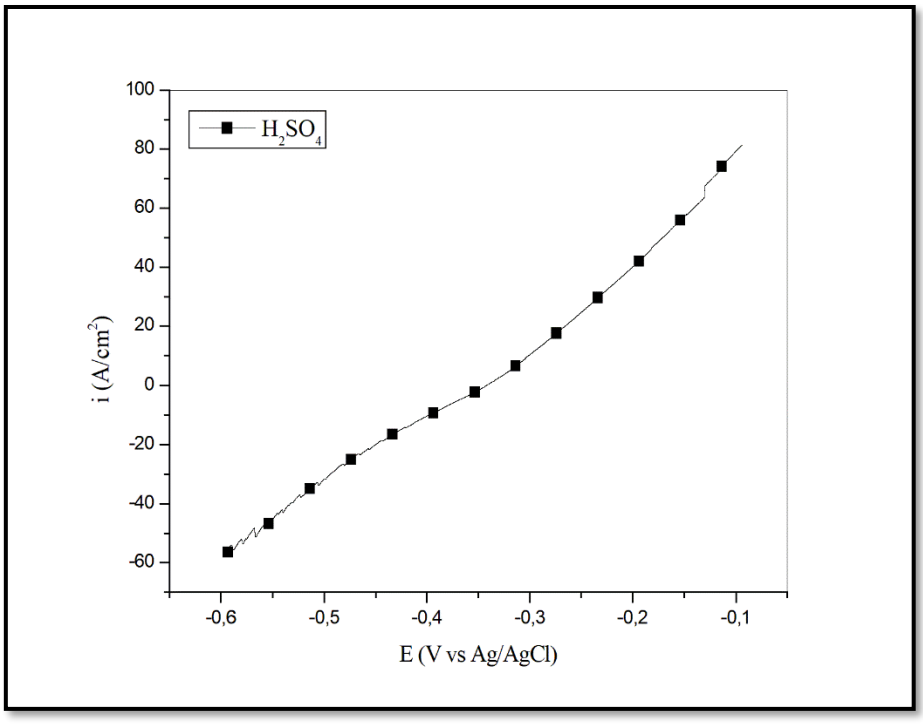

Figure III-1: linear Polarization curves of API 5L X70 carbon steel in 0.5M H_2SO_4 at 30°C.

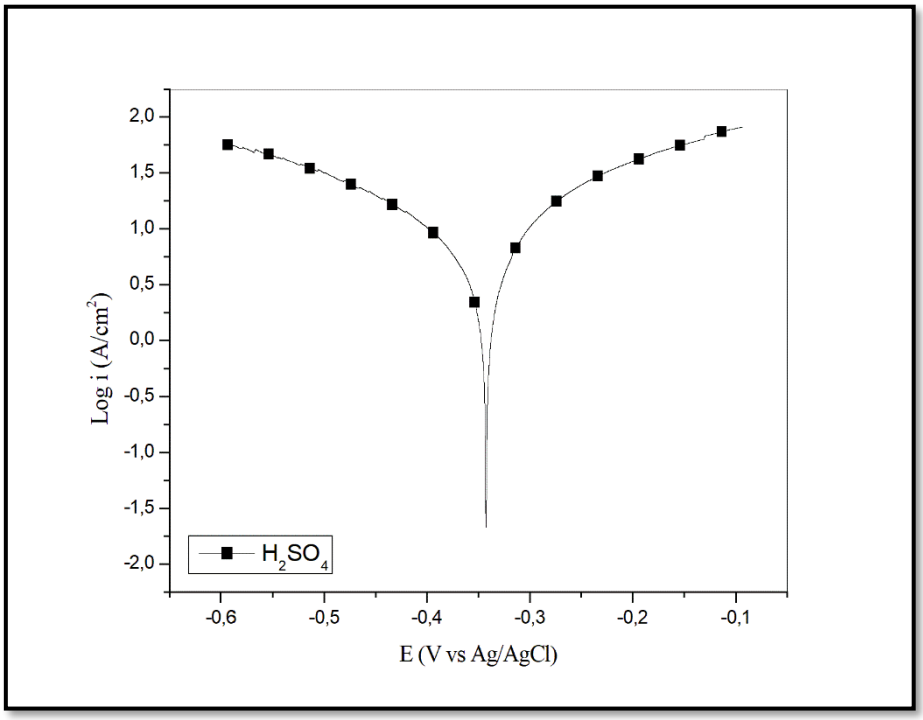

Figure III-2: logarithmic Polarization curves of API 5L X70 carbon steel in 0.5M H_2SO_4 at 30°C.

All values of the electrochemical parameters determined from the polarization test are summarized in table III-1.

Table III-1: Potentiodynamic polarization parameters for API 5L X70 in 0.5M H_2SO_4 solution at 30 °C.

Concentrations	Ecorr (mV)	Icorr (ε A $^{-2}$)c :	ba (mV dec^{-1})	bc (mV dec^{-1})
0.5M H_2SO_4	-342	7506	184	253

III.1.1.2 Electrochemical impedance spectroscopy technique

Figures (III-3 and III-4) represent the Nyquist plots diagram and Bode plots respectively; EIS has been achieved to determine different electrochemical parameters of API 5L X70 steel in 0.5M H_2SO_4 at 30°C and 1 hour of immersion time.

The table III-2 summarizes the electrochemical parameters obtained from electrochemical impedance spectroscopy of API 5L X70 steel in 0.5M H_2SO_4 solution.

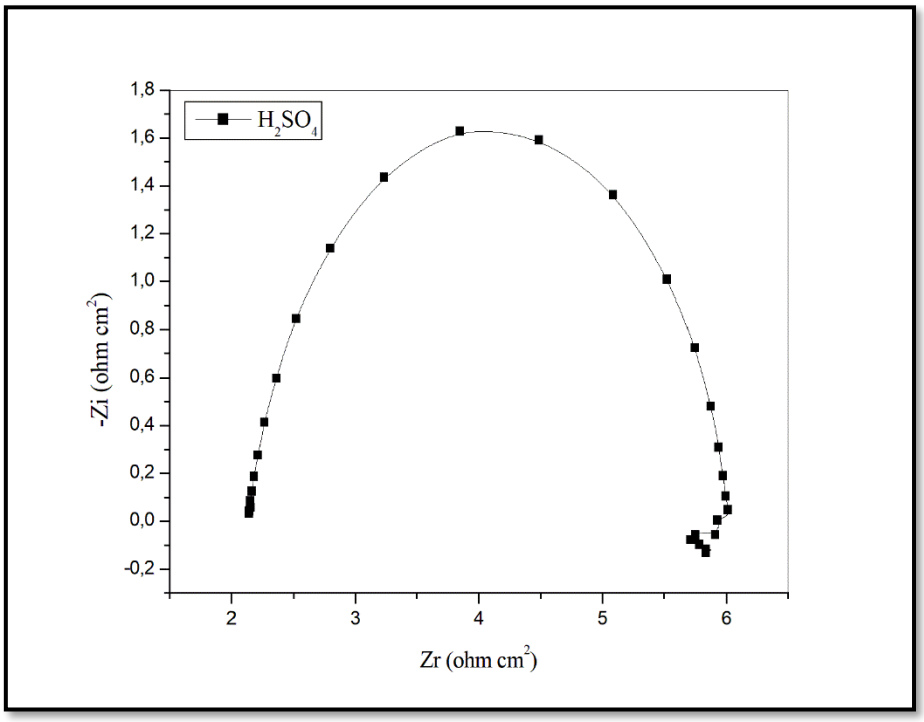

Figure III-3: Nyquist plots for API 5L X70 steel 0.5M H_2SO_4 at 30°C

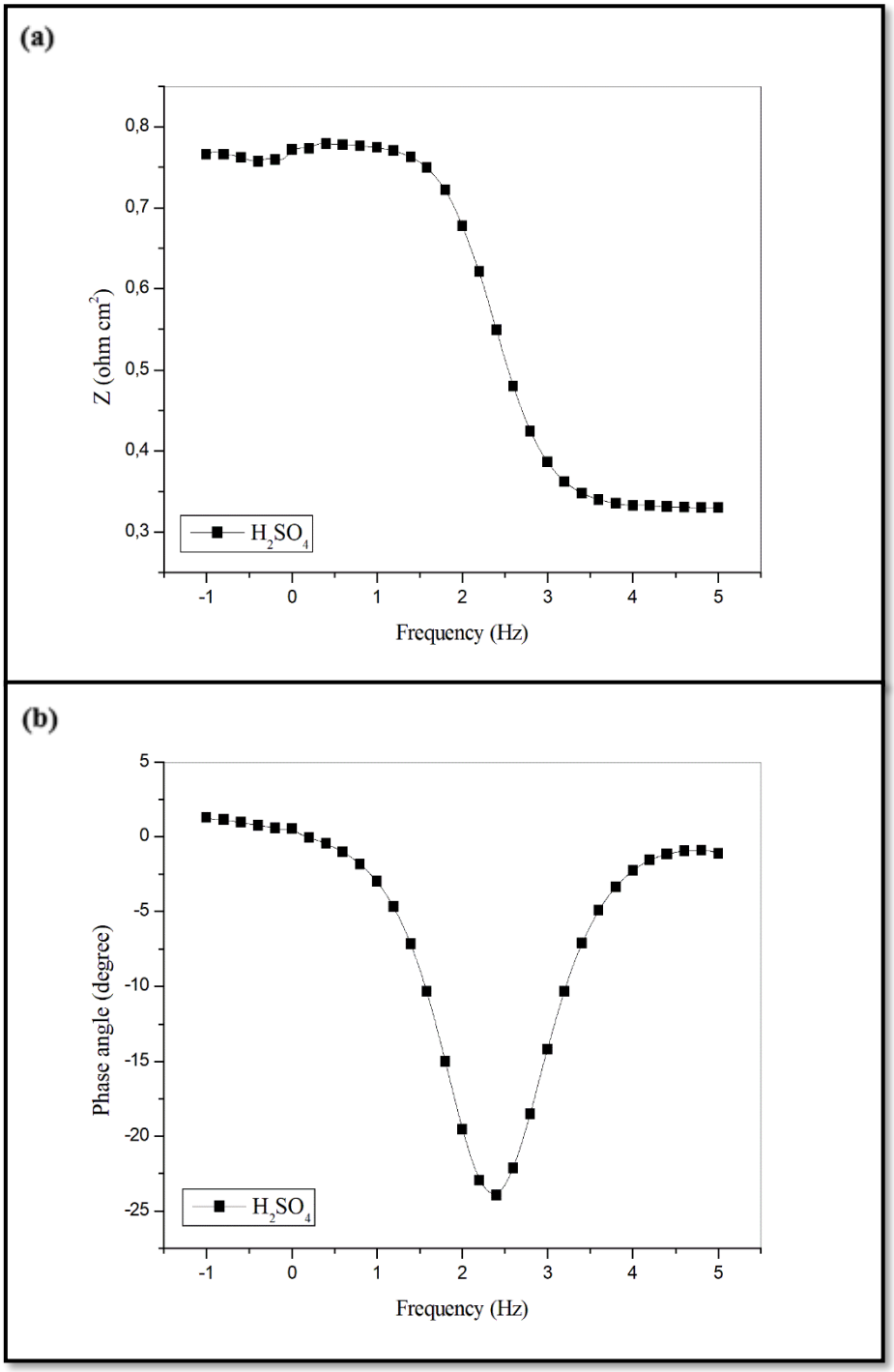

Figure III-4: Bode plots for API 5L X70 steel in 0.5M HCl and 0.5M H_2SO_4 at 30 °C (a) Bode modulus and (b) Bode phase angle.

Table III-2: Electrochemical impedance parameters for API 5L X70 in 0.5M H_2SO_4 solution at 30 ° C.

concentration	Rs (q ²)c	*Y0* (Õ q -²S) n	*n*	*Rt* (q ²)c	*L* (H cm²)	*RL* (q ²)c	η_{EIS} %
Blank	2,14	624.7	0.39	7,65	8 x10^{-5}	7.80	-

III.1.2 Immersion test of API 5L X70 steel in H_2SO_4 acid medium

An immersion test was conducted to examine the corrosion type of API 5L X70 steel after 72 hours of immersion in 0.5M H_2SO_4 medium. In order to analyze the surface, (OM) has been used after removing corrosion products by polishing the surface for 10 seconds with abrasive paper 1200 (Figure III-5).

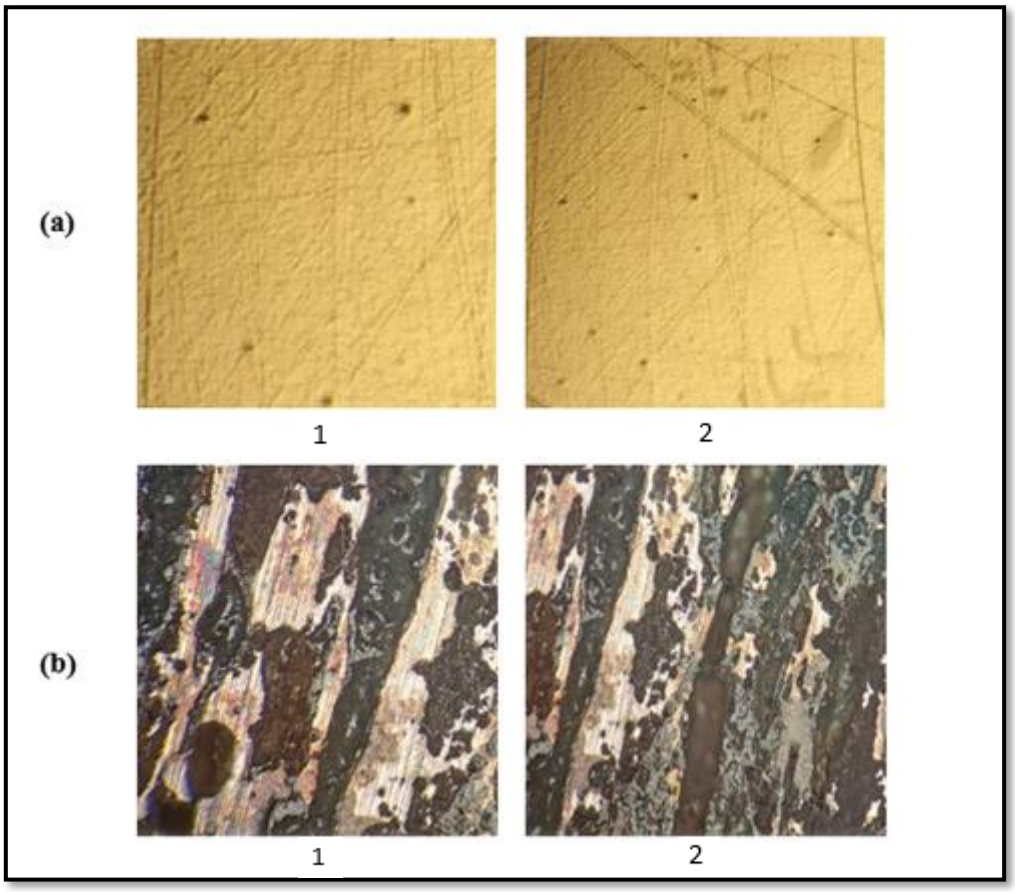

Figure III-5: OM images (x20) of the API 5L X70 steel surface after removing the corrosion products (a) before corrosion, (b) after immersion in 0.5M H_2SO_4 at 30°C for 72 h.

General corrosion (uniform corrosion) of carbon steel occurs. The corrosive attack occurs uniformly across the entire surface area, as well as pitting corrosion located on the majority of the surface area

According to figure III-5, the OM morphologies (b) of API 5L X70 steel were immersed in 0.5M H_2SO_4, and the surface of the specimens appear completely corroded due to oxidation and dissolution of the iron.

After immersion in 0.5M H_2SO_4 acid for one hour, the OM analyses on the API 5L X70 steel specimen agreed with the electrochemical impedance spectroscopy and potentiodynamic polarization results.

III.2 Part two: Effect of AVG on Inhibition Efficiency of API 5L X70 steel in 0.5M H_2SO_4 solution

in this part, Electrochemical techniques were used to determine the electrochemical parameters such as corrosion rate and inhibition efficiency in order to study the properties of AVG in 0.5M H_2SO_4, and Surface analysis to confirm the analysis results obtained from the electrochemical techniques.

III.2.1 Potentiodynamic polarization measurements of API 5L X70 steel in 0.5 M H_2SO_4 media

The effect of Aloe Vera Gel (AVG) on the anodic and cathodic behavior of API 5L X70 steel in 0.5M sulfuric acid solution has been studied by polarization measurements and the Tafel plots are shown in Figure (III-6 and III-7). The values of corrosion current density (I_{corr}), corrosion potential (E_{corr}), cathodic Tafel slope (b_c), anodic Tafel slope (b_a), and inhibition efficiency (i_{pol}) are presented in Table III-3.

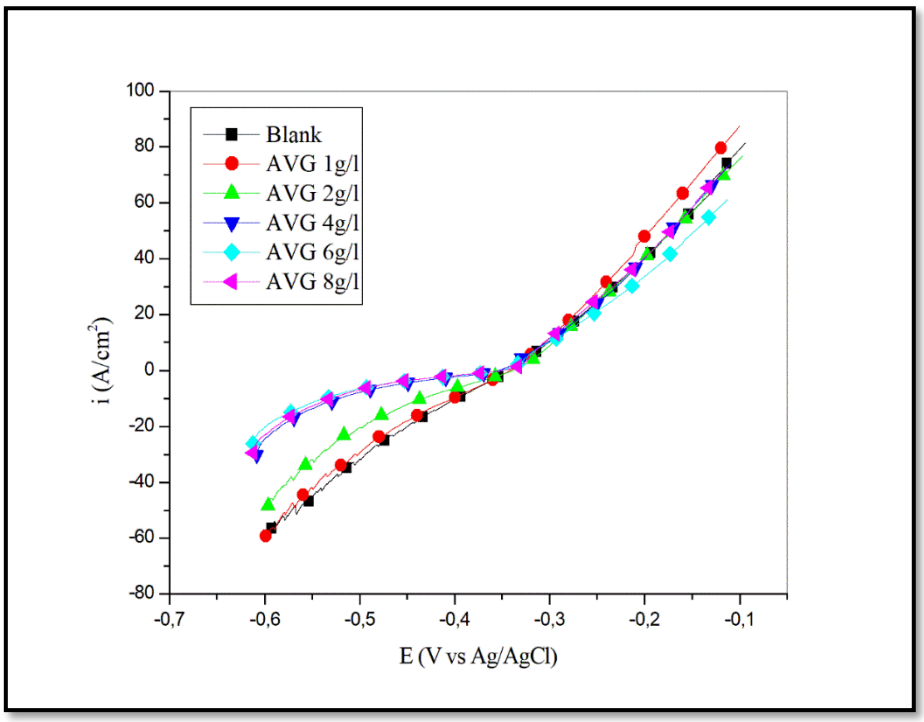

Figure III-6: linear Potentiodynamic polarization curves for API 5L X70 pipeline steel in 0.5M H_2SO_4 without and with different concentrations of AVG at 30 °C (immersion time is 1 h).

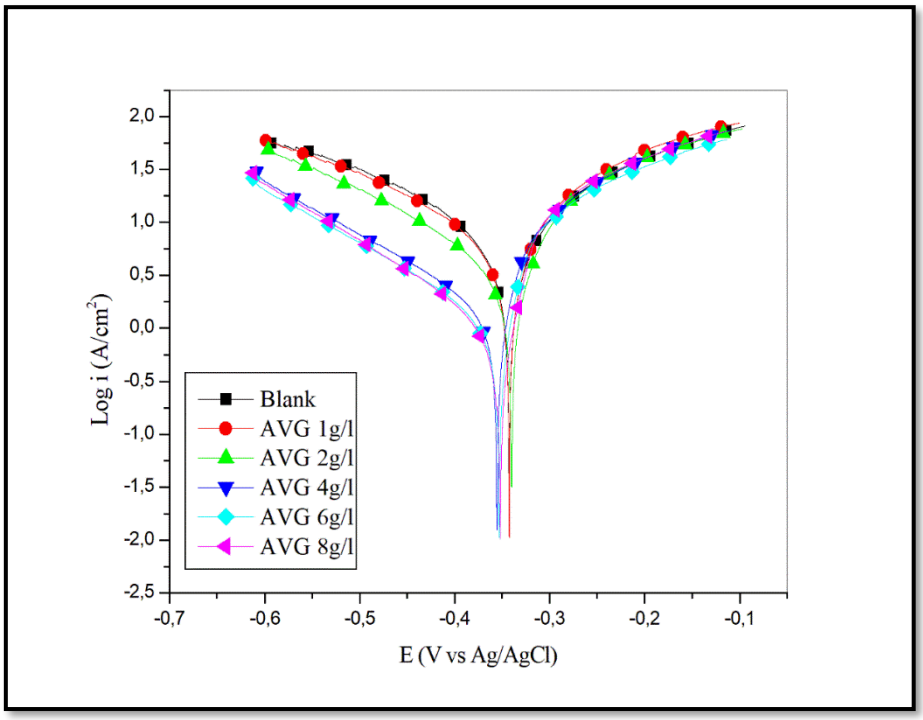

Figure III-7: logarithmic Potentiodynamic polarization curves for API 5L X70 pipeline steel in 0.5M H_2SO_4 without and with different concentrations of AVG at 30 °C (immersion time is 1 h).

In Figures (III-6 and III-7), both anodic and cathodic currents were inhibited, indicating that AVG suppressed both anodic and cathodic reactions, and by increasing the concentration of AVG, the anodic dissolution was reduced and the hydrogen evolution reaction was also retarded.

A summary of the values of various electrochemical parameters are listed in Table III-3. The table below provides values of corrosion parameters, such as the corrosion potential Ecorr, corrosion current density Icorr, Tafel slopes (bc, ba), and inhibition efficiency η_{pol} for steel corrosion in 0.5M H_2SO_4 with different concentrations of AVG.

Table III-3: Potentiodynamic polarization parameters for API 5L X70 in 0.5 M H_2SO_4 solution in the absence and the presence of different concentration of AVG at 30 °C.

Concentrations	Ecorr (mV)	Icorr (ε A $^{-2}$)c	ba (mV dec^{-1})	- bc (mV dec^{-1})	d_{pol} %
Blank	-342	7506	184	253	-
1 g/l AVG	-343	6163	138	229	17.89%
2 g/l AVG	-342	3725	104	210	50.37%
4 g/l AVG	-355	1606	59	200	78.60%
6 g/l AVG	-354	1171	49	196	84.39%
8 g/l AVG	-352	1001	45	177	86.66%

From Table III-3 it is evident that the corrosion current density (Icorr) value decreases from 7506 to 1001 ε A $^{-2}$c with the highest concentration of 8 g/l AVG. The addition of AVG does not alter the value of Ecorr significantly indicating the mixed type of inhibiting behavior of the inhibitor. In literature, it has been also reported that if the displacement in Ecorr is more than 85 mV the inhibitor can be seen as a cathodic or anodic type [63], and if the displacement is less than 85 mV, then the inhibitor may be regarded as mixed-type [64].

In our study, the displacement was less than 85mV indicating that AVG is a mixed inhibitor. Similar results were also reported with Dialkyldithiophosphate Derivative [65] and quinoxaline derivative [66].

From Table III-3, I_{corr} decreases while d_{pol} increases with the increase in inhibitor concentration. The maximum value of 86.66% of d_{pol} also indicates that AVG is a good inhibitor for API 5L X70 steel in 0.5M sulfuric acid. In addition, the results indicate that 4g/l AVG is the optimum inhibitor concentration for API 5L X70 in 0.5 M H_2SO_4 solution.

III.2.2 Electrochemical impedance spectroscopy measurements of API 5L X70 steel in 0.5 M H_2SO_4 media

Impedance measurements on API 5L X70 steel immersed in 0.5M sulfuric acid solution for 1h without and with different concentrations of AVG can be seen in Figures III-8, III-9 (Nyquist diagrams, and Bode plots).

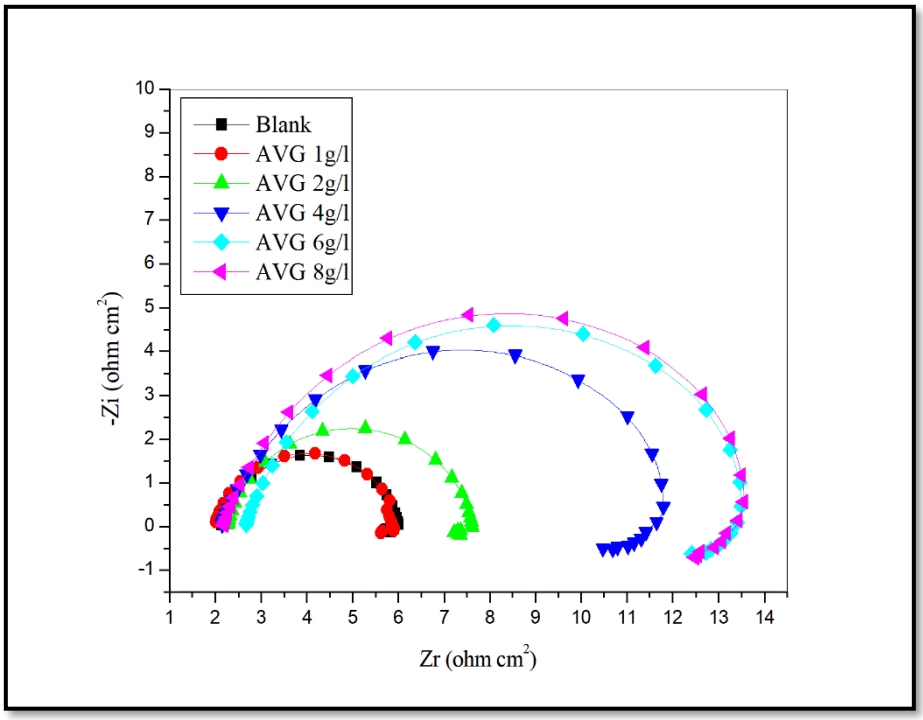

Figure III-8: Nyquist plots of the corrosion of API 5L X70 in 0.5M H_2SO_4 without and with different concentrations of AVG at 30 °C (immersion time is 1 h).

Nyquist plots showing identical shapes demonstrate that no significant modification arises in the mechanism of corrosion, as a consequence of adding inhibitor, implying that the presence of inhibitor in the solution did not stop the corrosion. However, the diameter of capacitive loops rises as the concentration of inhibitor increases, which is suggestive of slower charge transfer corrosion reactions [67].

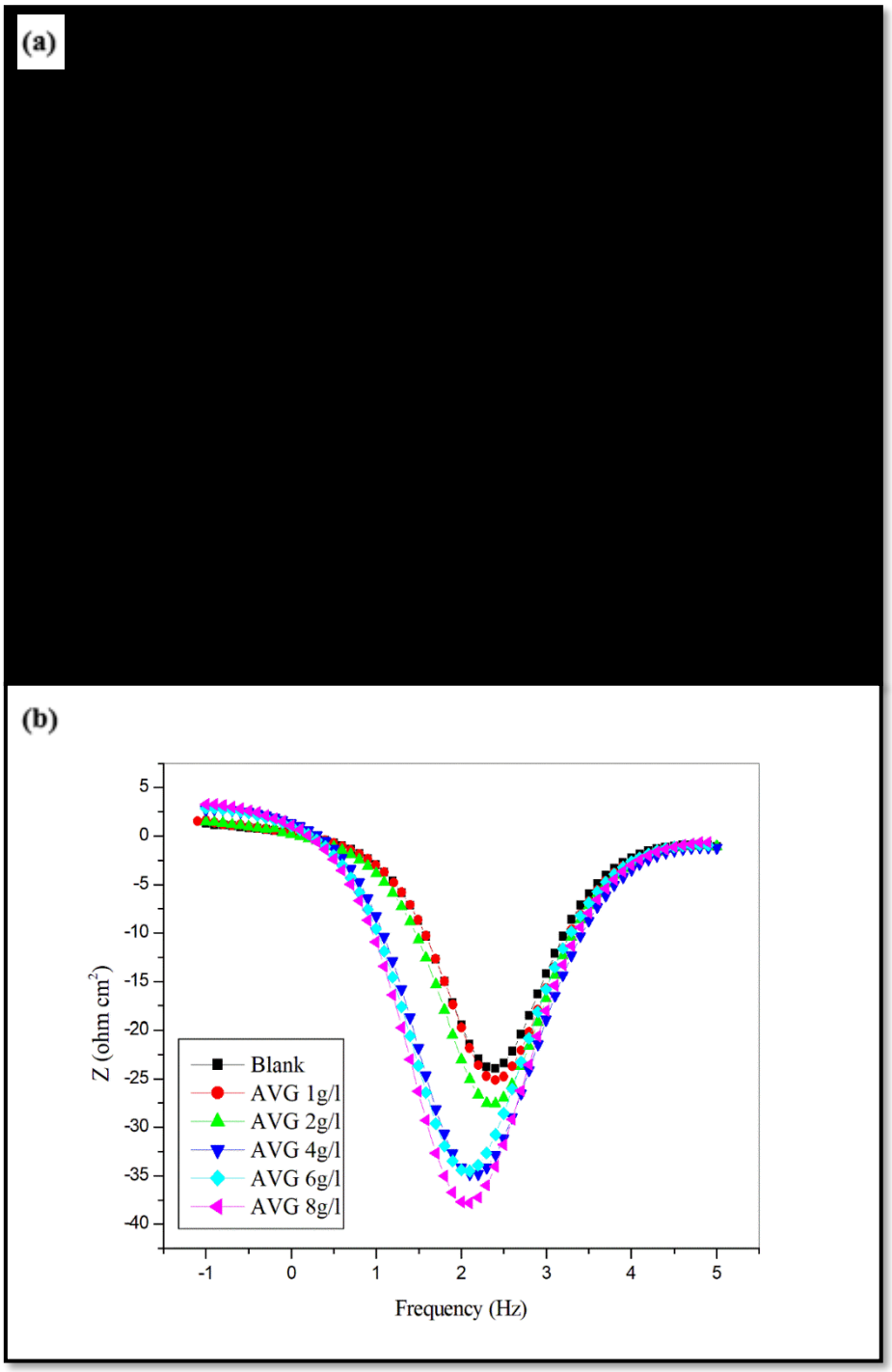

Figure III-9: Bode plots for API 5L X70 steel in 0.5M H_2SO_4 without and with different concentrations of AVG at 30 °C, (a)Bode modulus and (b) Bode phase angle.

The Nyquist plots reveal that each impedance diagram consists of a large capacitive loop at high frequencies (HF) and an inductive loop at low frequencies (LF) both in the absence and presence of inhibitor. The presence of two-time constants for iron dissolution at Ecorr in the absence of inhibitors has been reported in the literature [68].

The HF capacitive loop could be attributed to the double layer capacity in parallel with the charge transfer resistance (Rt). The LF inductive loop may be originated from the relaxation process obtained by adsorption species as H^{+}_{ads} and $SO4^{-2}$ on the surface of the metal. It may also be attributed to the re-dissolution of the passivated surface at low frequencies [69].

A model of equivalent circuit has been attempted to fit these experimental data using the software Impedance Model Editor designed by Gamry 7 Echem Analyst. Figure III-10 shows simulated and experimentally generated impedance diagrams for API5L X70 steel immersed in 0.5M sulfuric acid solution in the presence of 4 g/l AVG.

From the figure III-10, the measured impedance plot is in accordance with the one calculated by the equivalent circuit. The circuit consists of the solution resistance R_s, the charge transfer resistance R_t, the constant phase element (CPE), the inductive elements, R_L, and L.

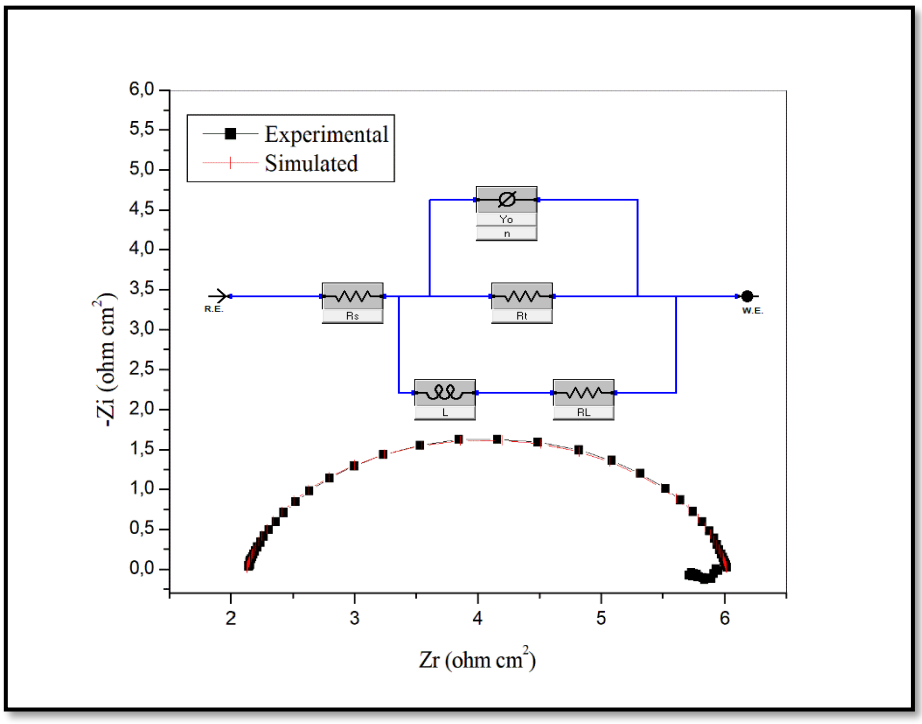

Figure III-10: Nyquist plot of experimental data and simulated data, together with the equivalent circuit used to fit the impedance data, recorded for API 5L X70 steel in 0.5M H_2SO_4 containing 4 g/l AVG.

Table III-4 shows representative parameter values of the fitting results to EIS data obtained for API 5L X70 steel using the equivalent circuits of figure III-10.

Table III-4: Electrochemical impedance parameters for API 5L X70 in 0.5 M H_2SO_4 solution in the absence and the presence of AVG at 30 ° C.

concentration	Rs (q 2)c	*Y*0 (Õ q -2S) n	*n*	*Rt* (q 2)c	*L* (H cm^2)	*RL* (q 2)c	η_{EIS} %
Blank	2,14	624.7	0.39	7,65	8 $x10^{-5}$	7.80	-
1 g/l AVG	1.96	615.9	0.38	8.97	9 $x10^{-5}$	7.16	14.71%
2 g/l AVG	2.27	537.2	0.88	15.35	1.3 $x10^{-4}$	8.25	50.16%
4 g/l AVG	2.16	458.4	0.90	34.26	8 $x10^{-5}$	13.8	77.67%
6 g/l AVG	2.64	659.6	0.85	45.47	1.2 $x10^{-4}$	15	83.17%
8 g/l AVG	2.19	653.5	0.86	53.80	7 $x10^{-4}$	15	85.78%

From the Table III-4, we can see clearly that the inhibition efficiencies from the impedance measurements are similar with those obtained from Potentiodynamic polarization.

III.2.3 OM analysis of the API 5L X70 steel immersion in H_2SO_4 acid medium with and without AVG

The API 5L X70 steel specimens has been immersed in the 0.5M H_2SO_4 acid solution in the absence and presence the of optimum concentration of inhibitor (4 g/L AVG) for 72 hours at 30°C, the specimens have been polished with abrasive paper (1200 grade) for 10 seconds to remove the corrosion products on steel surface and dried used for taking the image (figure III-11).

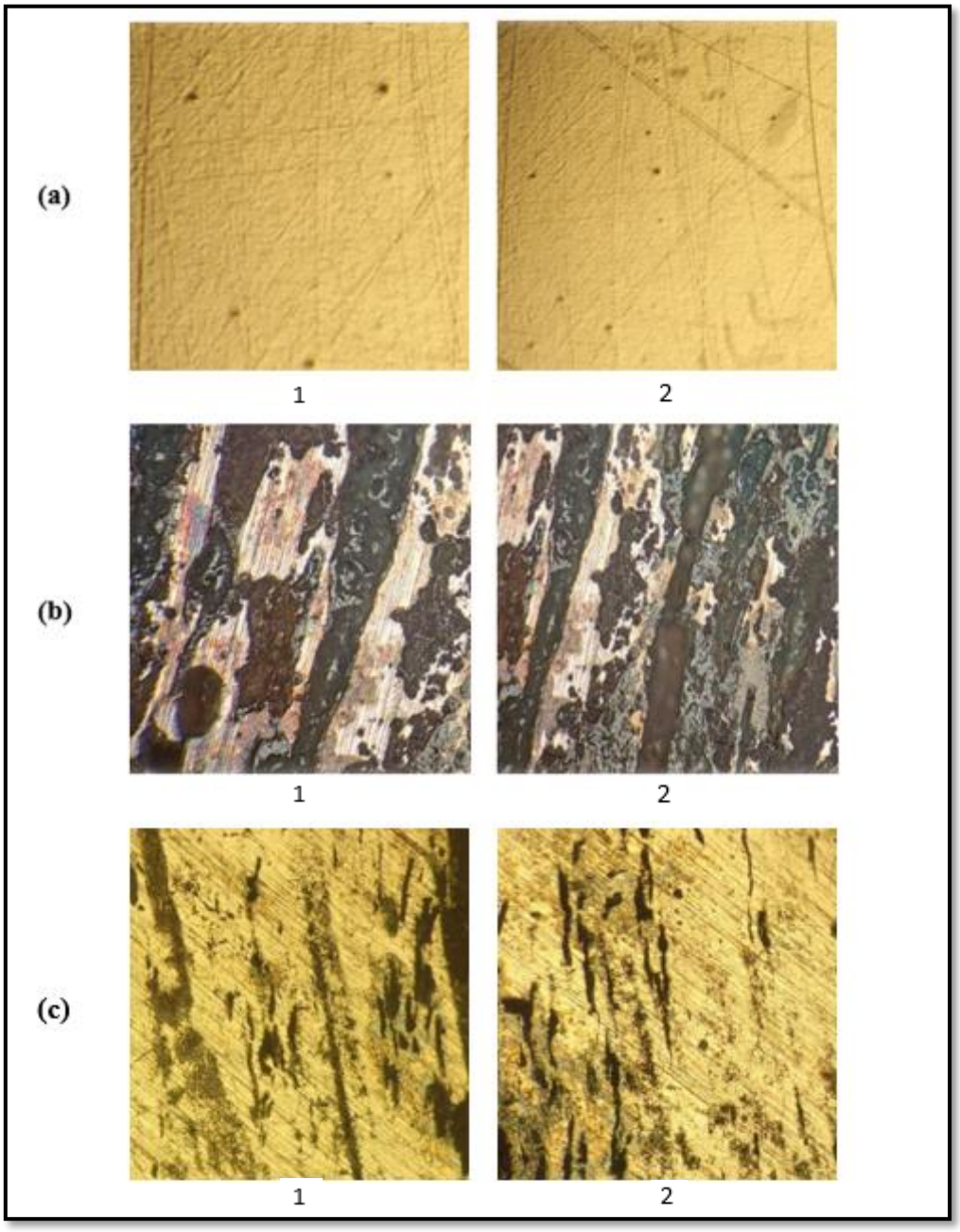

Figure III-11: OM images (x20) of the API 5L X70 steel surface after removing the corrosion products (a) before corrosion, (b) after immersion in 0.5M H_2SO_4, (c) after immersion in 0.5M H_2SO_4 + 4 g/L AVG at 30°C for 72 h

It is clear from the figure III-11 (b) that in the absence of AVG, API 5L X70's surface is completely damaged and the steel is dissolved due to an oxidation reaction with a generalized type of corrosion.

However, when the API 5L X70 steel was immersed in 0.5 M H_2SO_4 solution containing the optimized concentration 4 g/L of AVG (figure c), the specimen surface seems to be attacked but the degree of corrosion and dissolution is reduced.

These immersion test results are in agreement with those obtained using electrochemical impedance techniques.

III.3 Part three: Synergistic effect of Iodide ions and AVG for the corrosion inhibition of API 5L X70 steel in 0.5M H_2SO_4

The synergistic effect of iodide ions on inhibitive action of AVG in 0.5 M sulfuric acid solution was investigated by using different electrochemical techniques to determine the electrochemical parameters such as corrosion rate and corrosion potential with the concentration of inhibitor at 4 g/L AVG (the optimal concentration), OM have also been used to analyze to the surface of steel.

III.3.1 Potentiodynamic polarization measurements of API 5L X70 steel in 0.5M H_2SO_4 in the presence of AVG plus KI and in the absence of KI

The potentiodynamic polarization behavior of API 5L X70 steel in 0.5 M H_2SO_4, 4g/l AVG with 0.5mM KI and without KI is shown in Figure (III-12 and III-13). It is clear from the figure that the addition of AVG has reduced both the anodic iron dissolution and cathodic hydrogen evolution reactions. Corrosion current densities reduced markedly in the presence of 4g/L AVG + 0.5mM KI compared to 4g/L AVG only. The related electrochemical parameters such as Icorr, Ecorr, the cathodic Tafel slope (bc), and anodic Tafel slope (ba) obtained from the polarization curves are listed in Table III-4.

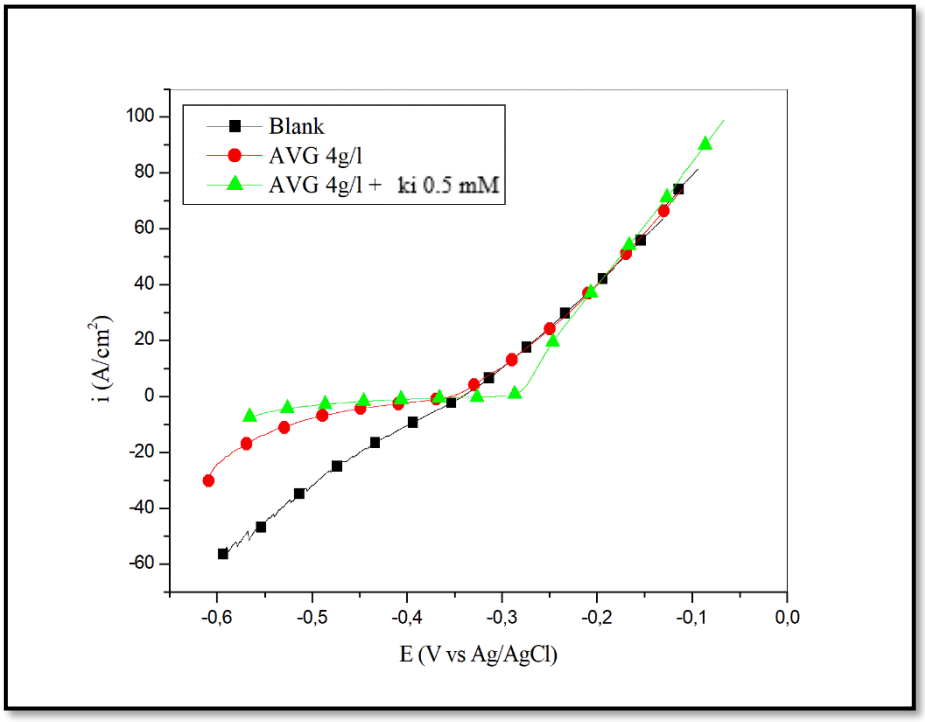

Figure III-12: linear Potentiodynamic polarization curves for API 5L X70 pipeline steel in 0.5M H_2SO_4 with 4g/l AVG + 0.5Mm KI and without KI at 30 °C (immersion time is 1 h).

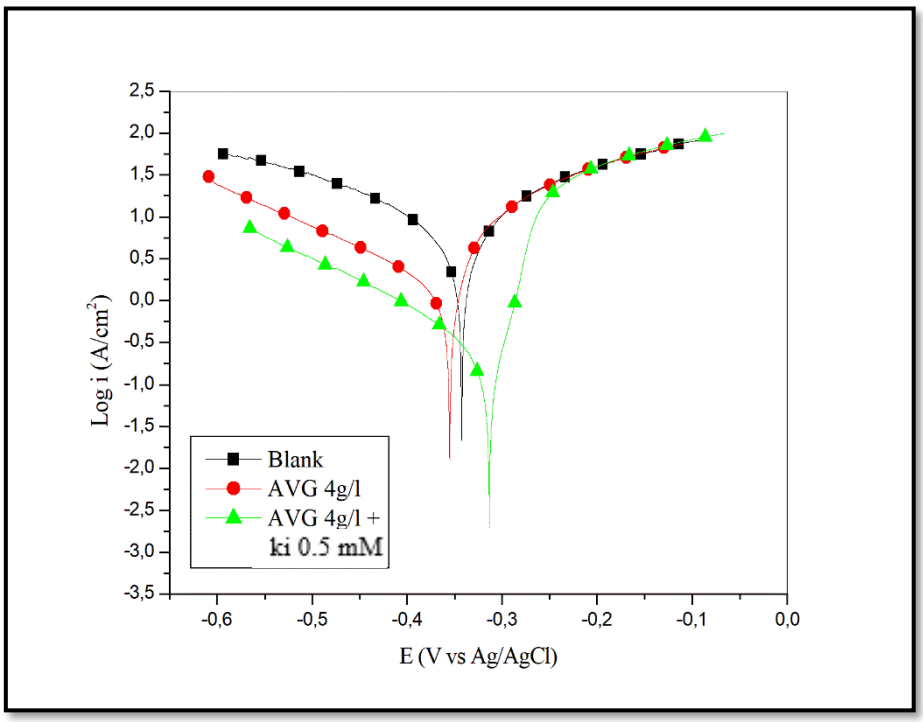

Figure III-13: logarithmic Potentiodynamic polarization curves for API 5L X70 pipeline steel in 0.5M H_2SO_4 with 4g/l AVG + 0.5Mm KI and without KI at 30 °C (immersion time is 1 h).

Table III-5: Potentiodynamic polarization parameters for API 5L X70 in 0.5 M H_2SO_4 solution with 4g/l AVG + 0.5Mm KI and without KI at 30 °C

Concentrations	Ecorr (mV)	Icorr (ε A $^{-2}$)c	ba (mV dec^{-1})	- bc (mV dec^{-1})	d_{pol} %
Blank	-342	7506	184	253	-
4 g/l AVG	-355	1606	59	200	78.60%
4 g/l AVG + 0.5mM KI	-312	213	29	139	97.16%

The results in the Table III-5 indicated that I_{corr} decreased significantly when 4g/L AVG was combined with 0.5mM KI. The E_{corr} values were not decreased that much (from -355 mV to -312 mV, less than 85 mV) in the presence of the combination of AVG + KI. Confirming that, the combination AVG + KI classified as a mixed-type inhibition.

The inhibition efficiency for the combination AVG with KI was calculated and also listed in the table. The addition of iodide ions (0.5 mM) has improved the value of IE% of 4g/l AVG (from 78.60% up to 97.16%).

Although the anodic and cathodic currents were significantly reduced when both AVG and KI were present, a low polarization current was observed, indicating that a synergistic effect has occurred between AVG and iodide ions. The anodic and cathodic Tafel slopes changed, indicating that the corrosion mechanism is changed [70].

III.3.2 Electrochemical impedance spectroscopy measurements of API 5L X70 steel in 0.5 M H_2SO_4 with 4g/l AVG + 0.5Mm KI and without KI

Impedance measurements on API 5L X70 steel immersed in 0.5M sulfuric acid solution for 1h with 4g/l AVG plus 0.5mM KI and without KI can be seen in Figures III-14, III-15 (Nyquist diagrams, and Bode plots).

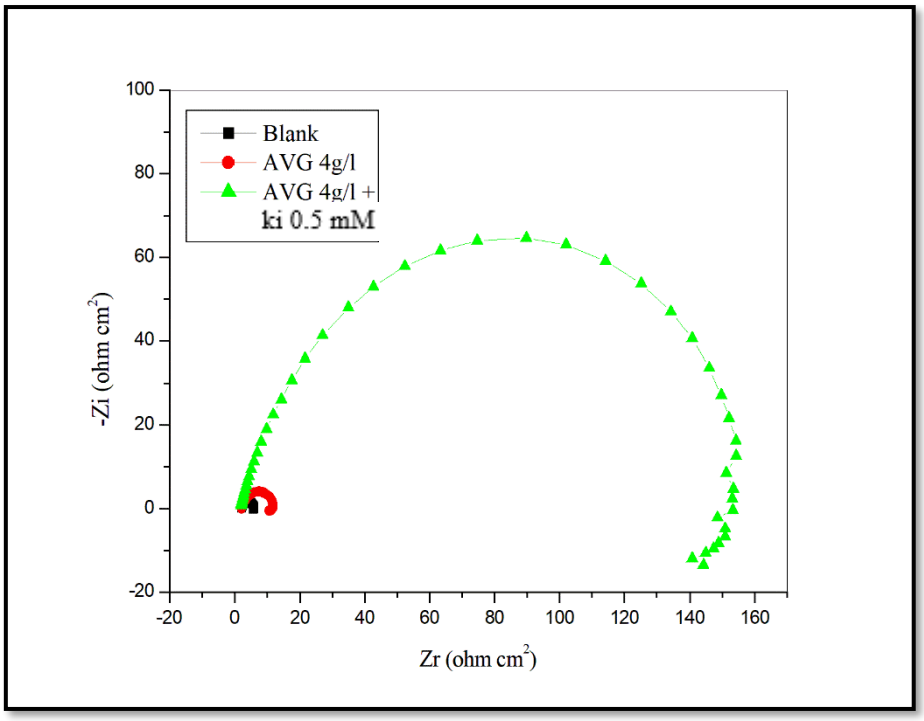

Figure III-14: Nyquist plots of the corrosion of API 5L X70 in 0.5M H_2SO_4 with 4g/l AVG plus 0.5mM KI and without KI at 30 °C (immersion time is 1 h).

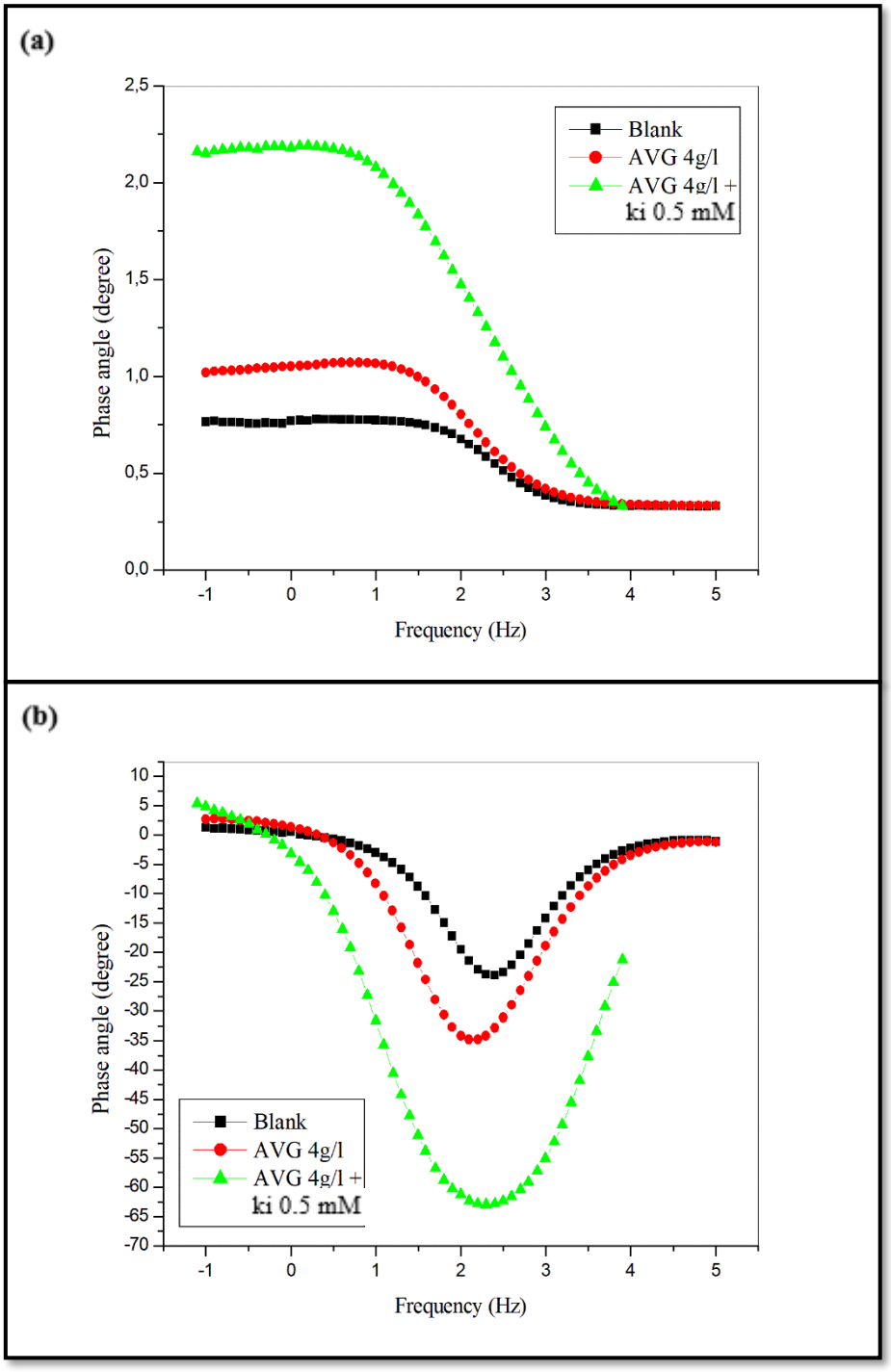

Figure III-15: Bode plots for API 5L X70 in 0.5M H_2SO_4 with 4g/l AVG plus 0.5mM KI and without KI at 30 °C, (a)Bode modulus and (b) Bode phase angle.

The high-frequency part of the impedance and phase angle describes the behavior of an inhomogeneous surface layer, whereas the low frequency component depicts the kinetic response for the charge transfer reaction [72]. It is observed that the combination of (AVG+ 0. 5 mM KI) results in an increase in the size of the semicircle in figure III-14, in the impedance of the interface in figure III-15 (a), and in the maximum phase angle in figure III-14 (b), which indicate inhibition of the corrosion process, the impedance spectra for the Nyquist plots were analyzed by fitting to the equivalent circuit model shown in figure III-11, which has been used previously to model the carbon steel/acid interface [73]. Table III-6 gives the values of the electrochemical impedance parameters.

Table III-6: Electrochemical impedance parameters for API 5L X70 in 0.5M H_2SO_4 solution with 4g/l AVG + 0.5 mM KI at 30 °C.

concentration	Rs (q 2)c	*Y*0 (Õ q -2S) n	*n*	*Rt* (q 2)c	*L* (H cm^2)	*RL* (q 2)c	η_{EIS} %
Blank	2,14	624.7	0.39	7,65	8 $x10^{-5}$	7.80	-
4 g/l AVG	2.16	458.4	0.90	34.26	8 $x10^{-5}$	13.8	77.67%
4 g/l AVG + 0.5mM KI	2.20	128.2	0.86	262	0.05	380	97.08%

The addition of KI to the 4g/l AVG further enhances Rt values (from 34.26Wcm^2 to 262Wcm^2) and the inhibition value from (77.67% to 97.08%) indicating that KI enhances the adsorption of AVG by of the synergistic effect of iodide ions.

III.3.3 OM analysis

The API 5L X70 steel specimens were immersed after been polished in the sulfuric acid solution for 72 hours immersion time in the absence and presence 4g/l AVG and 0.5 mM KI

the specimens have been polished with abrasive paper (1200 grade) to 10 seconds for removing the corrosion products on steel surface and dried used for taking the image (figure III-16)

Figure III-16 (b) represents the specimen immersion in 0.5M H_2SO_4 solution in absence of the inhibitor which is characterized by highly corroded and damaged surface. However, in the presence of 4 g/L AVG the surface morphologies of the specimen (figure III-16 c) have been improved owing to the formation of the protective film on the metallic surface, and in the presence of 4 g/L AVG + 0.5 mM KI the surface morphologies of the specimen (figure III-16 d) is remarkably better than in the presence of 4 g/L AVG indicating that synergy is improving the protection of the inhibitor

Based on immersion tests, these results confirm those obtained from the potentiodynamic polarization and impedance measurements.

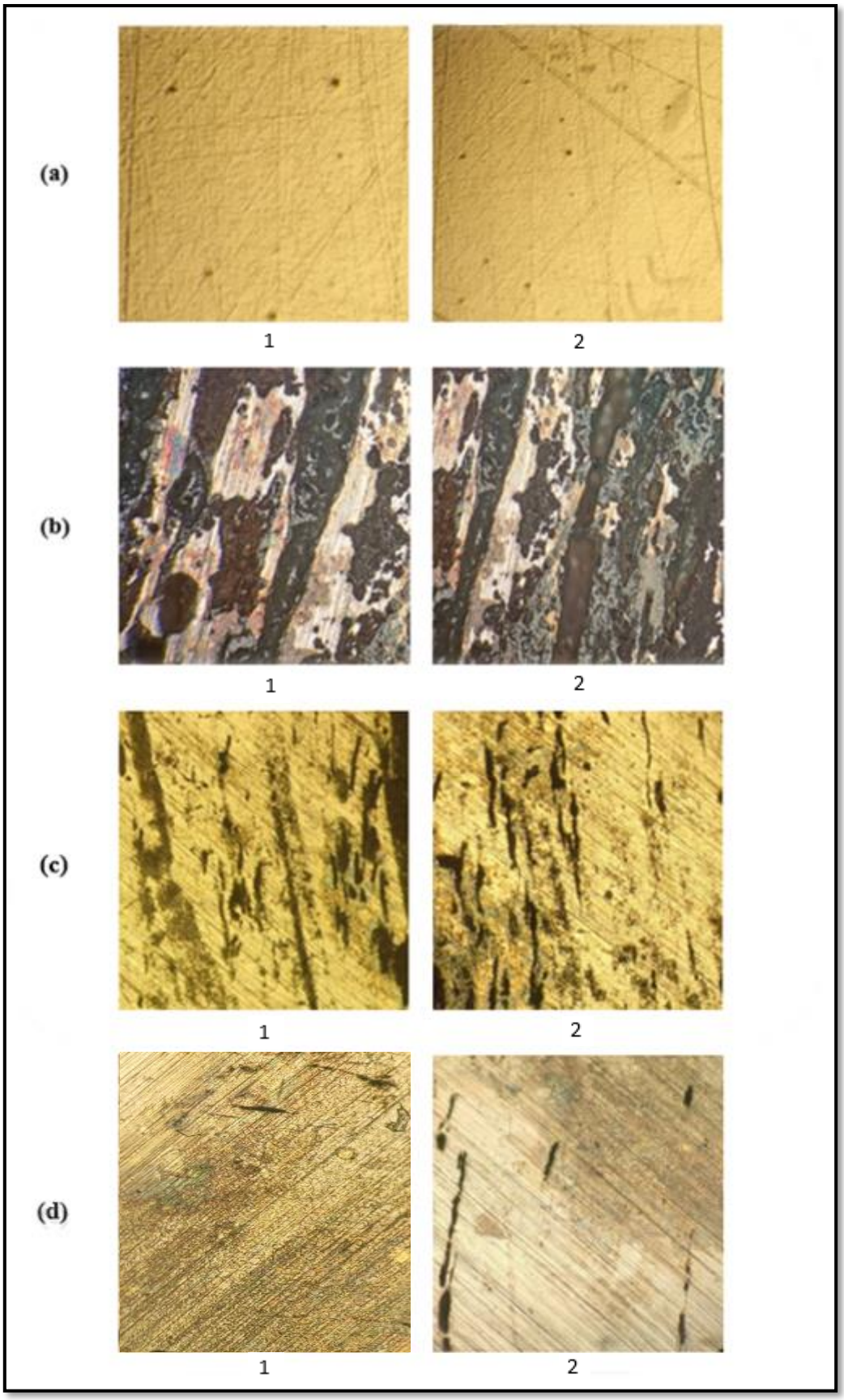

Figure III-16: OM images (x20) of the API 5L X70 steel surface after removing the corrosion products (a) before corrosion, (b) after immersion in 0.5M H_2SO_4, (c) after immersion in 0.5M H_2SO_4 + 4 g/L, (d) after immersion in 0.5M H_2SO_4 + 4 g/L AVG + 0.5 Mm KI at 30°C for 72

General Conclusion

The aim of this research was to analyze and evaluate a natural organic compound taken from a plant (Aloe Vera Gel) to determine its inhibition efficiency as an alternative to the toxic chemical inhibitors used in the petroleum industry.

The evaluation of Aloe Vera Gel (AVG) in 0.5M H_2SO_4 medium provided the following results, the potentiodynamic polarization data indicates that the inhibitor affects both cathodic and anodic processes, which means that the inhibitor acts as a mixed type and the corrosion rate of API 5L X70 $^{-2}$ in the absence of the and in presence of the optimum concentration (4g/L AVG) it decreases significantly to 16 ^{2}, and in the same time, the inhibi(η_{pol}) increases to reach the value of 78.60%. From the electrochemical impedance spectroscopy (EIS), the charge transfer resistance (Rt) increases with the increase of the concentration (Blank) of the 34.26 ^{2} (4 g/l AVG) and the inhibition efficiency (η_{EIS}) is 77.67% in the same concentration. From Optical Microscope (OM) images, the specimen is aggressively attacked in absence of AVG and in presence of 4g/L AVG the damage is reduced. Plus, the results obtained from the surface analysis are comforted those results of electrochemical impedance spectroscopy and potentiodynamic polarization.

The synergetic effect of iodide ions has been studied in 0.5M H_2SO_4 acid solution. From the potentiodynamic polarization, the inhibi(η_{pol}) is increased from 78.60% to 97.16% in the presence of 4 g/l AVG + 0.5mM KI, and addition has reduced both the anodic iron dissolution and the cathodic hydrogen evolution reactions. From the EIS, the value of inhibition efficiency (η_{EIS}) is increased from 77.67% to 97.08% in the presence of optimum concentration with KI. This can be attributed to the enhanced adsorption of AVG in the presence of KI because of the synergistic effect of iodide ions. From the OM micrograph of the API 5L X70 steel, the specimen immersion in 0.5M H_2SO_4 solution in the absence of the inhibitor is characterized as a highly corroded and damaged surface. However, in the presence of an optimum concentration (4 g/l AVG) plus KI, the surface of the specimen has been remarkably been better than in the presence of AVG only indicating that synergy is improving the protection of the inhibitor owing to the formation of the protective film on the metallic surface. These results have confirmed those obtained from the electrochemical techniques.

References

[01]. Bondada, V., Pratihar, D. K., & Kumar, C. S. (2018). Detection and quantitative assessment of corrosion on pipelines through image analysis. *Procedia Computer Science*, *133*, 804-811.

[02]. Koch, G. (2017). Cost of corrosion. *Trends in oil and gas corrosion research and technologies*, 3-30.

[03]. Robertson Jr, J. O., & Chilingarian, G. V. (1989). Acidizing Oilwells. In *Developments in Petroleum Science* (Vol. 19, pp. 161-190). Elsevier.

[04]. Mustafa, C. M., & Shahinoor Islam Dulal, S. M. (1996). Molybdate and nitrite as corrosion inhibitors for copper-coupled steel in simulated cooling water. *Corrosion*, *52*(1), 16-22.

[05]. Winkler, D. A., Breedon, M., White, P., Hughes, A. E., Sapper, E. D., & Cole, I. (2016). Using high throughput experimental data and in silico models to discover alternatives to toxic chromate corrosion inhibitors. *Corrosion Science*, *106*, 229-235.

[06]. Ahmad, A., Kumar, R., & Kumar, A. (2019). Effect of sodium molybdate and sodium tungstate in concrete rebar corrosion. *Anti-Corrosion Methods and Materials*.

[07]. Zhang, Y., Zhang, S., Tan, B., Guo, L., & Li, H. (2021). Solvothermal synthesis of functionalized carbon dots from amino acid as an eco-friendly corrosion inhibitor for copper in sulfuric acid solution. *Journal of Colloid and Interface Science*, *604*, 1-14.

[08]. Bharatiya, U., Gal, P., Agrawal, A., Shah, M., & Sircar, A. (2019). Effect of corrosion on crude oil and natural gas pipeline with emphasis on prevention by eco-friendly corrosion inhibitors: a comprehensive review. *Journal of Bio-and Tribo-Corrosion*, *5*(2), 1-12.

[09]. Gece, G. (2011). Drugs: A review of promising novel corrosion inhibitors. *Corrosion Science*, *53*(12), 3873-3898.

[10]. Odewunmi, N. A., Umoren, S. A., & Gasem, Z. M. (2015). Watermelon waste products as green corrosion inhibitors for mild steel in HCl solution. *Journal of Environmental Chemical Engineering*, *3*(1), 286-296.

[11]. Sedik, A., Lerari, D., Salci, A., Athmani, (2020). Dardagan Fruit extract as eco-friendly corrosion inhibitor for mild steel in 1 M HCl: Electrochemical and surface morphological studies. *Journal of the Taiwan Institute of Chemical Engineers*, *107*, 189-200.

[12]. Bentrah, H., Rahali, Y., & Chala, A. (2014). Gum Arabic as an eco-friendly inhibitor for API 5L X42 pipeline steel in HCl medium. *Corrosion Science*, *82*, 426-431.

[13]. Zhang, X., Li, W., Zuo, X., Tan, B., Xu, C., & Zhang, S. (2021). Investigating the inhibitive effect of Davidia involucrata leaf extract as a biological eco-friendly inhibitor for copper in acidic medium. *Journal of Molecular Liquids*, *325*, 115214.

[14]. Wang, Q., Tan, B., Bao, H., Xie, Y., Mou, Y., Li, P., ... & Yang, W. (2019). Evaluation of Ficus tikoua leaves extract as an eco-friendly corrosion inhibitor for carbon steel in HCl media. *Bioelectrochemistry*, *128*, 49-55.

[15]. Spennemann, D. (2015). *Techniques in Historic Preservation: Why do corroded corrugated iron roofs have a striped appearance?* (ILWS Report; No. 93). Charles Sturt University.

[16]. Salunkhe, P. B., & Rane, S. P. (2016). Treatise on conducting polymers for corrosion protectionï Advanced approach. Paint India, 61.

[17]. Virtanen, S. (2011). Corrosion and passivity of metals and coatings. In Tribocorrosion of passive metals and coatings (pp. 3-28). Woodhead Publishing.

[18]. Zavareh, M. A., Sarhan, A. A. D. M., Abd Razak, B. B., & Basirun, W. J. (2014). Plasma thermal spray of ceramic oxide coating on carbon steel with enhanced wear and corrosion resistance for oil and gas applications. Ceramics International, 40(9), 14267-14277.

[19]. Barreto, L. S., Tokumoto, M. S., Guedes, I. C., Melo, H. G. D., Amado, F. D. R., & Capelossi, V. R. (2017). Evaluation of the anticorrosion performance of peel garlic extract as corrosion inhibitor for ASTM 1020 carbon steel in acidic solution. *Matéria (Rio de Janeiro), 22*.

[20]. Bentrah, H., & CHALA, A. (2015). Corrosion des ouvrages pétroliers : Utilisation de la gomme arabique comme inhibiteur environnemental pour l'acier API 5L X42. *Université Mohamad Khider, BISKRA, Doctorat*.

[21]. Brusseau, M. L., & Chorover, J. (2019). Chemical processes affecting contaminant transport and fate. In *Environmental and Pollution Science* (pp. 113-130). Academic Press.

[22]. Kvarekvål, J., & Moloney, J. (2017). Sour corrosion. *Trends in Oil and Gas Corrosion Research and Technologies*, 113-147.

[23]. Obot, I. B., Solomon, M. M., Umoren, S. A., Suleiman, R., Elanany, M., Alanazi, N. M., & Sorour, A. A. (2019). Progress in the development of sour corrosion inhibitors: Past, present, and future perspectives. Journal of Industrial and Engineering Chemistry, 79, 1-18.

[24]. Ossai, C. I. (2012). Advances in asset management techniques: An overview of corrosion mechanisms and mitigation strategies for oil and gas pipelines. *International Scholarly Research Notices, 2012*.

[25]. Singh, A., Lin, Y., Ansari, K. R., Quraishi, M. A., Ebenso, E. E., Chen, S., & Liu, W. (2015). Electrochemical and surface studies of some Porphines as corrosion inhibitor for J55 steel in sweet corrosion environment. Applied Surface Science, 359, 331-339.

[26]. Popoola, L. T. (2019). Organic green corrosion inhibitors (OGCIs): a critical review. Corrosion Reviews, 37(2), 71-102.

[27]. Askari, M., Aliofkhazraei, M., & Afroukhteh, S. (2019). A comprehensive review on internal corrosion and cracking of oil and gas pipelines. *Journal of Natural Gas Science and Engineering*, *71*, 102971.

[28]. Popoola, L. T., Grema, A. S., Latinwo, G. K., Gutti, B., & Balogun, A. S. (2013). Corrosion problems during oil and gas production and its mitigation. *International Journal of Industrial Chemistry*, *4*(1), 1-15.

[29]. Askari, M., Aliofkhazraei, M., & Afroukhteh, S. (2019). A comprehensive review on internal corrosion and cracking of oil and gas pipelines. *Journal of Natural Gas Science and Engineering*, *71*, 102971.

[30]. GÜNER, M., & ÖZBAYER, M. M. (2019). Wear and its effects in centrifugal pumps. *Yüzüncü Yıl Üniversitesi Tarım Bilimleri Dergisi*, *29*(3), 569-582.

[31]. Raja, P. B., Ismail, M., Ghoreishiamiri, S., Mirza, J., Ismail, M. C., Kakooei, S., & Rahim, A. A. (2016). Reviews on corrosion inhibitors: a short view. *Chemical Engineering Communications*, *203*(9), 1145-1156.

[32]. Perez, T. E. (2013). Corrosion in the oil and gas industry: an increasing challenge for materials. *Jom*, *65*(8), 1033-1042.

[33]. Heakal, F. E. T., & Elkholy, A. E. (2017). Gemini surfactants as corrosion inhibitors for carbon steel. *Journal of Molecular Liquids*, *230*, 395-407.

[34]. Basulto, G. K. P., Carrillo, I., Ortega, D., Martinez, L., & Cantó, J. (2015). Evaluation at Pipeline Corrosion at Oil Field. *ECS Transactions*, *64*(26), 103.

[35] *Acidizing - Treatment in Oil and Gas Operators: Briefing paper.* American Petroleum Institute (API) 2014.

[36]. Alcalá, L. M. (2012). Acid stimulation of geothermal wells in Mexico, El Salvador and The Philippines. *REVISTA MEXICANA DE GEOENERGÍA· ISSN 0186 5897*, 17.

[37]. Singh, A., & Quraishi, M. A. (2015). Acidizing corrosion inhibitors: a review. *J. Mater. Environ. Sci*, *6*(1), 224-235.

[38]. Al-Mahasneh, M., Al Rabadi, S., & Khaswaneh, H. (2021). Assessment of oil-producing wells by means of stimulation approach through matrix acidizing: a case study in the Azraq region. *Journal of Petroleum Exploration and Production Technology*, *11*(9), 3479-3491.

[39]. Shafiq, M. U., & Mahmud, H. B. (2017). Sandstone matrix acidizing knowledge and future development. *Journal of Petroleum Exploration and Production Technology*, *7*(4), 1205-1216.

[40]. Kalfayan, L. J., & Metcalf, A. S. (2000, October). Successful sandstone acid design case histories: exceptions to conventional wisdom. In *SPE Annual Technical Conference and Exhibition*. OnePetro.

[41]. TAOUI, H. (2020). *Protection against corrosion of API 5L X70 carbon steel intended to petroleum industry by green inhibitor: SchinusMolle Resin as an eco-friendly inhibitor* (Doctoral dissertation, Université Mohamed Khiderï Biskra).

[42]. Mular, A. L., Halbe, D. N., & Barratt, D. J. (Eds.). (2002). *Mineral processing plant design, practice, and control: proceedings* (Vol. 1). SME.

[43]. Aliofkhazraei, M. (Ed.). (2014). *Developments in corrosion protection*. BoDï Books on Demand.

[44]. Kesavan, D., Gopiraman, M., & Sulochana, N. (2012). Green inhibitors for corrosion of metals: a review. Chem. Sci. Rev. Lett, 1(1), 1-8.

[45]. Emregül, K. C., Düzgün, E., & Atakol, O. (2006). The application of some polydentate Schiff base compounds containing aminic nitrogens as corrosion inhibitors for mild steel in acidic media. *Corrosion Science*, *48*(10), 3243-3260.

[46]. Sayin, K., & Karakaк, D. (2013). Quantum corrosion inhibitors. *Corrosion science*, *77*, 37-45.

[47]. Goyal, M., Kumar, S., Bahadur, I., Verma, C., & Ebenso, E. E. (2018). Organic corrosion inhibitors for industrial cleaning of ferrous and non-ferrous metals in acidic solutions: A review. *Journal of Molecular Liquids*, *256*, 565-573.

[48]. Ituen, E., Akaranta, O., & James, A. (2017). Evaluation of performance of corrosion inhibitors using adsorption isotherm models: an overview. *Chem. Sci. Int. J*, *18*(1), 1-34.

[49]. Abbasov, V. M., Abd El-Lateef, H. M., Aliyeva, L. I., Qasimov, E. E., Ismayilov, I. T., & Khalaf, M. M. (2013). A study of the corrosion inhibition of mild steel C1018 in CO2-saturated brine using some novel surfactants based on corn oil. *Egyptian Journal of Petroleum*, *22*(4), 451-470.

[50]. Aljamali, N. M., Aldujaili, R. A. B., & Alfatlawi, I. O. (2021). Physical and Chemical Adsorption and its Applications.

[51]. Nandiyanto, A. B. D., Girsang, G. C. S., Maryanti, R., Ragadhita, R., Anggraeni, S., Fauzi, F. M., ... & Al-Obaidi, A. S. M. (2020). Isotherm adsorption characteristics of carbon microparticles prepared from pineapple peel waste. *Communications in Science and Technology*, *5*(1), 31-39.

[52]. Chigondo, M., & Chigondo, F. (2016). Recent natural corrosion inhibitors for mild steel: an overview. *Journal of Chemistry*, *2016*.

[53]. Alï Asadi, A. A., Abdullah, A. S., Khaled, N. I., & Alkhafaja, R. J. (2015). Effect of an Aloe Vera as a Natural Inhibitor on The Corrosion of Mild Steel in 1 wt.% NaCl. Int J Eng Technol, 2(06).

[54]. Ahl, L. I. (2019). Polysaccharide Diversity Across the Genus Aloe (Doctoral dissertation, University of Copenhagen, Faculty of Science, Natural History Museum of Denmark).

[55]. Al-Turkustani, A. M., Arab, S. T., & Al-Dahiri, R. H. (2010). Aloe plant extract as environmentally friendly inhibitor on the corrosion of aluminum in hydrochloric acid in absence and presence of iodide ions. Modern Applied Science, 4(5), 105.

[56]. Sobhy, M. A., Abbas, M., & El-Zomrawy, A. A. (2021). Evaluation of Aloe vera Gel extract as eco-friendly corrosion inhibitor for carbon steel in 1.0 M HCl. *Egyptian Journal of Chemistry*, *64*(11), 5-6.

[57]. Ribeiro, D. V., & Abrantes, J. C. C. (2016). Application of electrochemical impedance spectroscopy (EIS) to monitor the corrosion of reinforced concrete: A new approach. *Construction and Building Materials*, *111*, 98-104.

[58]. Berradja, A. (2019). Electrochemical techniques for corrosion and tribocorrosion monitoring: Methods for the assessment of corrosion rates. *Corrosion Inhibitors*.

[59]. Haldhar, R., Prasad, D., & Saxena, A. (2018). Myristica fragrans extract as an eco-friendly corrosion inhibitor for mild steel in 0.5 M H2SO4 solution. *Journal of Environmental Chemical Engineering*, *6*(2), 2290-2301.

[60]. Okonkwo, P. C., Belgacem, I. B., Ige, O. O., Emori, W., Uzoma, P. C., Eqbal, M. O., & Bhowmik, H. (2021). Potentiodynamic polarization test as a versatile tool for bipolar plates materials at start-up and shut-down environments: a review. *International Journal of Green Energy*, *18*(11), 1193-1202.

[61]. Di Gianfrancesco, A. (2017). Technologies for chemical analyses, microstructural and inspection investigations. In *Materials for ultra-supercritical and advanced ultra-supercritical power plants* (pp. 197-245). Woodhead Publishing.

[62]. Zhu, Y., Wang, L., Behnamian, Y., Song, S., Wang, R., Gao, Z., ... & Xia, D. H. (2020). Metal pitting corrosion characterized by scanning acoustic microscopy and binary image processing. *Corrosion Science*, *170*, 108685.

[63]. Manssouri, M., El Ouadi, Y., Znini, M., Costa, J., Bouyanzer, A., Desjobert, J. M., & Majidi, L. (2015). Adsorption proprieties and inhibition of mild steel corrosion in HCl solution by the essential oil from fruit of Moroccan Ammodaucus leucotrichus. *J. Mater. Environ. Sci*, *6*(3), 631-646.

[64]. Bourazmi, H., Tabyaoui, M., Hattabi, L., El Aoufir, Y., & Taleb, M. (2018). Methanolic extract of Salvia officinalis plant as a green inhibitor for the corrosion of carbon steel in 1 M HCl. *J. Mater. Environ. Sci*, *9*, 928-938.

[65]. Su, X., Lai, C., Peng, L., Zhu, H., Zhou, L. S., Zhang, L., ... & Zhang, W. (2016). A dialkyldithiophosphate derivative as mild steel corrosion inhibitor in sulfuric acid solution. *Int. J. Electrochem. Sci*, *11*, 4828-4839.

[66]. Tayebi, H., Bourazmi, H., Himmi, B., El Assyry, A., Ramli, Y., Zarrouk, A., ... & Hammouti, B. (2014). Combined electrochemical and quantum chemical study of new quinoxaline derivative as corrosion inhibitor for carbon steel in acidic media. *Der Pharma Chem*, *6*(5), 220-234.

[67]. Umoren, S. A., Solomon, M. M., Ali, S. A., & Dafalla, H. D. (2019). Synthesis, characterization, and utilization of a diallylmethylamine-based cyclopolymer for corrosion mitigation in simulated acidizing environment. *Materials Science and Engineering: C*, *100*, 897-914.

[68]. Djellab, M., Bentrah, H., Chala, A., & Taoui, H. (2019). Synergistic effect of halide ions and gum arabic for the corrosion inhibition of API5L X70 pipeline steel in H2SO4. *Materials and Corrosion*, *70*(1), 149-160.

[69]. Qian, B., Wang, J., Zheng, M., & Hou, B. (2013). Synergistic effect of polyaspartic acid and iodide ion on corrosion inhibition of mild steel in H2SO4. *Corrosion Science*, *75*, 184-192.

[70]. Fouda, A. E. A. S., Al-Zehry, H. H., & Elsayed, M. (2018). Synergistic effect of potassium iodide with Cassia italica extract on the corrosion inhibition of carbon steel used in cooling water systems in 0.5 M H2SO4. *Journal of Bio-and Tribo-Corrosion*, *4*(2), 1-17.

[71]. Khaled, K. F., & Hackerman, N. (2003). Investigation of the inhibitive effect of ortho-substituted anilines on corrosion of iron in 1 M HCl solutions. *Electrochimica Acta*, *48*(19), 2715-2723.

[72]. Oguzie, E. E. (2010, March). Evaluation of the inhibitive effect of some plant extracts on the acid corrosion of mild steel. In *CORROSION 2010*. OnePetro.

[73]. Kissi, M., Bouklah, M., Hammouti, B., & Benkaddour, M. (2006). Establishment of equivalent circuits from electrochemical impedance spectroscopy study of corrosion inhibition of steel by pyrazine in sulphuric acidic solution. *Applied surface science*, *252*(12), 4190-4197.

Abstract:

The corrosion inhibition properties of Aloe Vera gel (AVG) as an Eco-friendly inhibitor on API 5L X70 carbon steel in 0.5M sulfuric acid (H_2SO_4) solution has been examined and characterized by potentiodynamic polarization and electrochemical impedance spectroscopy (EIS) methods. These methods were complemented with Optical Microscope (OM) examinations of the electrode surface. The experimental results reveal that the inhibitor has a good inhibiting effect on the API 5L X70 carbon steel in 0.5M H_2SO_4 solution. The protection efficiency increases with increasing inhibitor concentration. Also, the synergetic effect between the iodine ions (I^-) and the inhibitor (AVG) has been studied. The potentiodynamic polarization data indicates that the inhibitor affects both cathodic and anodic processes, which means that the inhibitor acts as a mixed type. The surface analysis results also show a high inhibition efficiency of the Aloe Vera Gel on the steel surface (API 5L X70). Therefore, there is a great agreement between the results of electrochemical techniques and the results of surface analysis.

Keywords:

Aloe Vera gel, API 5L X70 carbon steel, Eco-friendly inhibitor, electrochemical techniques, OM, sulfuric acid.

الملخص:

تم فحص خصائص تثبيط التآكل لهلام الألو فيرا (AVG) كمثبط صديق للبيئة على الفولاذ الكربوني X70 في محلول 0.5 M من حامض الكبريتيك مستخدمين طريقة منحنيات الاستقطاب و عن طريق منحنيات نيكويست و بود . تم استكمال هذا البحث مع فحوصات المجهر الضوئي لسطح العينات. كشفت النتائج التجريبية أن المانع له تأثير تثبيطي جيد على الفولاذ الكربوني X70 في محلول 0,5M H2SO4.تزداد كفاءة الحماية مع زيادة تركيز المانع. كما تمت دراسة التأثير التآزري بين أيون اليود (I^-) والمثبط (AVG) .تشير بيانات منحنيات الاستقطاب إلى أن المثبط يؤثر على كل من التفاعلات الكاثودية والأنودية، مما يعني أن المثبط AVG يعمل كمثبط ذو تأثير مختلط. تظهر نتائج تحليل السطح أيضًا كفاءة تثبيط عالية لهلام الألو فيرا على سطح الفولاذ X70 لذلك، هناك اتفاق كبير بين نتائج التقنيات الكهروكيميائية ونتائج تحليل السطح.

الكلمات المفتاحية:

الألوة فيرا، مثبط صديق للبيئة، الفولاذ، تقنيات الكهروكيميائية، المجهر الضوئي، حامض الكبريتيك.